Standardなもの、Standardになり得るものとは

Adjuvant and Neoadjuvant Chemotherapy

7 卵巣癌

恩田貴志（国立がんセンター中央病院婦人科）

Point

- 進行卵巣癌においては、病変の局在に応じて直腸切除、結腸切除、脾摘、腹膜切除、虫垂切除、全大網切除、骨盤および大動脈リンパ節郭清術などが腫瘍縮小の目的で行われ、primary debulking surgery（PDS）とよばれる。
- PDSにおいて、optimal surgeryが可能であれば、optimal surgeryが達成できなかったsuboptimal症例に比べて予後の改善が期待できる。
- 現時点ではパクリタキセル（PTX：175～185mg/m^2、3時間投与）とカルボプラチン（CBDCA：AUC 5-6）の併用療法（TC療法）を3週ごとに6～9コース行うことが、進行卵巣癌に対する標準化学療法とされている。
- 進行卵巣癌に対してneoadjuvant chemotherapy（NAC）を行った後に、腫瘍縮小手術（interval debulking surgery；IDS）を行い、術後さらに追加で化学療法を行う治療（NAC療法）に期待がもたれるようになった。
- Retrospective studyでの比較や、prospectiveな第Ⅱ相試験の結果からは、NAC療法は期待される治療ではあるが、現時点ではあくまでも試験的治療であり、臨床試験以外では、治療開始時に手術を行うことが困難な全身状態の症例や、臨床的に腫瘍縮小手術不可能と判断される症例のみが対象となると考えられる。

卵巣癌の標準治療

卵巣癌に対する治療は、手術療法と化学療法から成り立っている。現在の標準治療は、まず初めに開腹手術を行い、術後に化学療法（adjuvant chemotherapy）を行う方法である。

1. 腫瘍縮小手術（primary debulking surgery）

最初に行う手術の目的は、卵巣癌であることを確認すること（組織学的診断）、病変の拡がりを確

報告者	year	median survival	
		optimal症例	suboptimal症例
Hacker	1983	18M	6M
Vogl	1983	>40M	16M
Delgado	1984	45M	16M
Pohl	1984	45M	16M
Conte	1985	>25M	14M
Posada	1985	>30M	18M
Louie	1986	24M	15M
Redman	1986	37M	26M
Neijt	1987	40M	21M
Hainsworth	1988	72M	13M
Piver	1988	48M	21M
Sutton	1989	45M	23M
Bertelson	1990	30M	18M
Eisenkop	1992	31M	18M
Michel	1996	24M	14M

表1 進行卵巣癌におけるoptimal surgeryと予後(文献2より引用)

認すること(進行期診断)、さらに進行卵巣癌で腹腔内や後腹膜リンパ節に転移を認める場合には、可能な限りの転移病巣を切除すること(腫瘍縮小)である。Ⅰ/Ⅱ期の早期癌においても必須の単純子宮全摘+両側付属器切除+部分大網切除術に加えて、進行癌においては、病変の局在に応じて直腸切除、結腸切除、脾摘、腹膜切除、虫垂切除、全大網切除、骨盤および大動脈リンパ節郭清術などが腫瘍縮小の目的で行われ、primary debulking surgery (PDS) とよばれる。

腫瘍縮小手術により、腫瘍の体積を減少し症状の緩和が得られることのほか、腫瘍の血流が不良で抗癌剤が到達しにくい部分や、血流不良で細胞分裂の低下した部分を少なくし、後の抗癌剤に対する感受性を向上させること、また腫瘍全体での細胞分裂の数を減らすことにより、耐性細胞の出現の機会を少なくすることなどの利点があると考えられている。

2. 腫瘍縮小手術後の残存腫瘍径

1975年にGriffiths[1]が、初回手術後の最大残存腫瘍径が予後と関連することを報告して以来、多くの報告によりその事実が確認され、進行卵巣癌の予後因子としてPDS後の最大残存腫瘍径が最も重要と考えられている。PDSにおいて、optimal surgery(残存腫瘍<0.5cm～残存腫瘍<3cmとさまざまな定義が用いられるが、近年は残存腫瘍<1cmが用いられる)が可能であれば、optimal surgeryが達成できなかったsuboptimal症例に比べて予後の改善が期待できる(**表1**)[2]。理論的には、Ⅲ/Ⅳ期の進行卵巣癌では、残存腫瘍のない完全切除はまれ、根治には化学療法の奏効が必要であるが、直径1cmを超える腫瘍を化学療法で消滅させることは困難であるためと考えられている。初回に侵襲の大きな腫瘍縮小手術を行うことは、重篤な合併症が多く、周術期死亡が7%にも起こりうることが報告されている(**表2**)が、optimal

報告者	報告年	症例数	重篤な合併症の発症率	手術に関連した死亡率
Hacker	1983	47	47%	3%
Chen	1985	84	67%	1%
Heintz	1986	70	44%	3%
Eisenkop	1992	263	34%	6%
Jänicke	1992	30	53%	NA
Venesmaa	1992	264	67%	2%
Guidozzi	1994	30	43%	7%
LoCoco	1995	129	8%	1%
Van Dam	1996	40	68%	3%
Michel	1997	152	33%	1%
Eisenkop	1998	163	42%	2%

NA：not available

表2 進行卵巣癌に対する初回腫瘍縮小手術の重篤な合併症（文献4より引用）

報告者	報告年	症例数	optimal surgery達成率
Neijt	1987	191	51%
Bertelson	1990	360	24%
Le Bouëdec	1990	180	26%
Hoskins	1992	925	41%
Del Campo	1994	91	27%
Venesmaa	1994	104	48%
Petit	1996	101	55%

表3 進行卵巣癌におけるoptimal surgery（文献5より引用）

surgeryが得られれば予後の改善が期待できることが、最初に腫瘍縮小手術を行う現在の標準治療の根拠となっている。進行卵巣癌における予後因子を解析したmeta-analysisによる報告では、optimal surgeryの達成率が最も重要な予後因子であり、進行卵巣癌全体の治療成績は、optimal surgeryの達成率が10%増加すれば、生存期間中央値で5.5%延長するとされている[3]。しかしながら、進行卵巣癌におけるoptimal surgeryの達成率は、きわめてaggressiveな施設において婦人科腫瘍専門医がPDSを行った報告では、50～90%程度の報告も認められるが、多施設での報告や、婦人科腫瘍専門医以外によるPDSでは、多くが50%に満たないのが現状である[4,5]（表3）。

3. 術後化学療法（adjuvant chemotherapy）

卵巣癌の化学療法は、1970年代～1990年代にかけての白金製剤やタキサン系薬剤の導入などにより、高い奏効率が期待できるようになった。現在、シスプラチン（CDDP）、カルボプラチン（CBDCA）などの白金製剤とパクリタキセル（PTX）、ドセタキセル（DTX）などのタキサン系薬剤の2剤併用療法が主として行われており、現時点ではPTX（175～185mg/m^2、3時間投与）とCBDCA

(AUC 5-6)の併用療法(TC療法)を3週ごとに6～9コース行うことが、進行卵巣癌に対する標準化学療法とされている。TC療法の卵巣癌初回治療における有効性に関して、各国で行われた第Ⅰ-Ⅱ相試験の結果、奏効率は79％(70～100％)、完全奏効率は57％(24～83％)と良好な成績が報告されている。

4. 進行卵巣癌の予後と治療戦略

侵襲の大きな初回腫瘍縮小手術、および化学療法剤の進歩にもかかわらず、進行卵巣癌の治療成績は満足のいくものではなく、FIGO (International Federation of Gynecology and Obstetrics)の2003年の報告によれば、ⅢA、ⅢB、ⅢC、Ⅳ期の5年生存率はそれぞれ、49％、41％、29％、13％[9]であった。進行卵巣癌の予後改善に向けて、新規抗癌剤や分子標的治療薬の導入、多剤併用療法における併用薬剤の変更、追加、末梢血幹細胞移植や骨髄移植を併用した高用量化学療法、腹腔内投与などの投与経路の変更、術前化学療法(neoadjuvant chemotherapy；NAC)の有用性などが種々の臨床試験により検討されている。進行癌のなかでも比較的早期の癌に対しては、腹腔内投与の化学療法の有用性が検討されているが、とりわけ進行した癌に対しては、NAC療法に期待が持たれている。

卵巣癌におけるNAC療法

1. NAC療法の利点

卵巣癌に対する化学療法の進歩を背景として、進行卵巣癌に対してneoadjuvant chemotherapy：NACを行った後に、腫瘍縮小手術(interval debulking surgery：IDS)を行い、術後さらに追加で化学療法を行う治療(NAC療法)に期待がもたれるようになった。

NAC療法の利点として、

①化学療法を先行することにより(手術枠の確保や他科との連携を要する手術先行に比べて)、速やかに治療を開始することが可能である。

②腫瘍や胸水、腹水によるPSの低下をNACにより改善し、また治療開始時にしばしばみられる血栓症の改善も期待でき、最初にPDSを行うより安全に侵襲の大きな手術を行いうる。

③NACによる腫瘍量、範囲の減少により、PDSを行う場合に比べて、他臓器合併切除の頻度が減少し、また(術式を拡大しなくても)optimal surgeryや根治性の高い手術の可能性が高くなることが期待でき、同時に重篤な合併症の減少も期待できる。

などの利点がある。

進行卵巣癌においては、NAC療法によって治療成績および患者のQOL(quality of life)の改善が期待される。

2. NAC療法と標準治療の比較成績

進行卵巣癌におけるNAC療法と標準治療の治療成績を比較した報告を紹介する(表4)。

Vergoteら[7]は、進行卵巣癌症例を対象として、切除可能性を試験開腹あるいは腹腔鏡により判断し、切除可能例には標準治療、不能例にはNAC療法を行うという方針で治療を行った1989～1997年の治療成績を、NAC療法導入以前の、全例に標準治療を行うという治療方針で治療を行った1980～1988年の治療成績と比較した。NAC療法導入後の3年生存率は42％で、NAC療法導入以前の3年生存率26％に比して、有意に($p = 0.0001$)予後良好であった。手術手技や化学療法剤の進歩も関連している可能性も否定できないが、NAC療法の有用性を示す結果である。

Kuhnら[5]は、多量の腹水貯留(＞500mL)を認める進行卵巣癌症例を対象に、NAC療法(31例)と標準治療(32例)のnon-randomizedの第Ⅱ相比較試験を行った。NAC療法群では84％、標準療

報告者（報告年）	治療法	予後の比較			NAC群の選択基準
		3年生存率	5年生存率	生存期間中央値	
Onnis	標準治療(n=284)	31%	21%		胸水/肝転移/腸管播種の有無など
(1996)	NAC療法(n=88)	27%	19%		によりNAC群を決定
	有意差	NS	NS		
Vergote	NAC導入前(n=112)	26%			切除可能性を試験開腹あるいは
(1998)	NAC導入後(n=173)	42%			腹腔鏡により判断し、切除不能例
	有意差	p=0.0001			にNAC療法
Schwartz	標準治療(n=206)			2.18Y	全身状態/合併症により手術不能
(1999)	NAC療法(n=59)			1.07Y	な症例、画像診断(CT)により腫瘍
	有意差			NS	切除不能と評価した例にNAC療法
Kayikçgioğlu	標準治療(n=158)		24%	38M	胸水貯留例、肝転移例、切除不能
(2001)	NAC療法(n=45)		30%	34M	が予想される多発転移症例や全身
	有意差		NS	NS	状態不良例にNAC療法
Kuhn	標準治療(n=32)			23M	同意が得られた例にNAC療法(無
(2001)	NAC療法(n=31)			42M	作為ではない、前向きの第Ⅱ相試
	有意差			p=0.007	験)

NS：Not significan

表4 進行卵巣癌に対する、NAC療法と標準治療の治療成績

法群では63％と、NAC療法群では、標準治療群に比して有意に(p＝0.04)高率にoptimal surgeryが達成できた。また、NAC療法群の生存期間中央値は、42ヵ月で、標準治療群の23ヵ月と比較して有意(p=0.007)に予後良好であった。

そのほか、Onnisら[9]、Kayikçioğluら[10]、Schwartzら[11]は、初回に腫瘍縮小手術が不能、あるいは全身状態のため手術不能で、結果的に術前化学療法となった症例をNAC療法群として標準治療群と比較した。NAC療法群はⅢ/Ⅳ期症例のなかでもより進行した症例、PSあるいは年齢などの条件が悪い予後不良群を対象としての比較であるが、NAC療法群は標準治療群に比較して、生存率において有意に劣ることはなかった。

これらの結果から、NAC療法は進行卵巣癌に対する新たな標準治療として、検討に値する治療と考えられる。

3. NAC療法の問題点

NAC療法は、進行卵巣癌治療において期待される治療ではあるが、NAC療法にも種々の問題点が挙げられる。

①最初にstaging laparotomyを兼ねたPDSを行わないため、対象疾患の診断が不正確となる可能性がある。したがって、消化器癌や乳癌などの転移を十分に除外したうえで、CT、MRIなどの画像診断で確実にⅢ-Ⅳ期の進行卵巣癌と診断される症例をNAC療法の対象とする必要がある。他臓器癌の転移が否定できない場合や、Ⅰ-Ⅱ期癌の可能性が否定できない場合には、診断確認のための開腹術や腹腔鏡が必須である。

②化学療法の効果が得られなければ、腫瘍縮小手術の機会を逸したり、optimal surgeryが達成できる可能性が減少したりする可能性がある。

③腫瘍量の多い状態で化学療法を行うため、薬

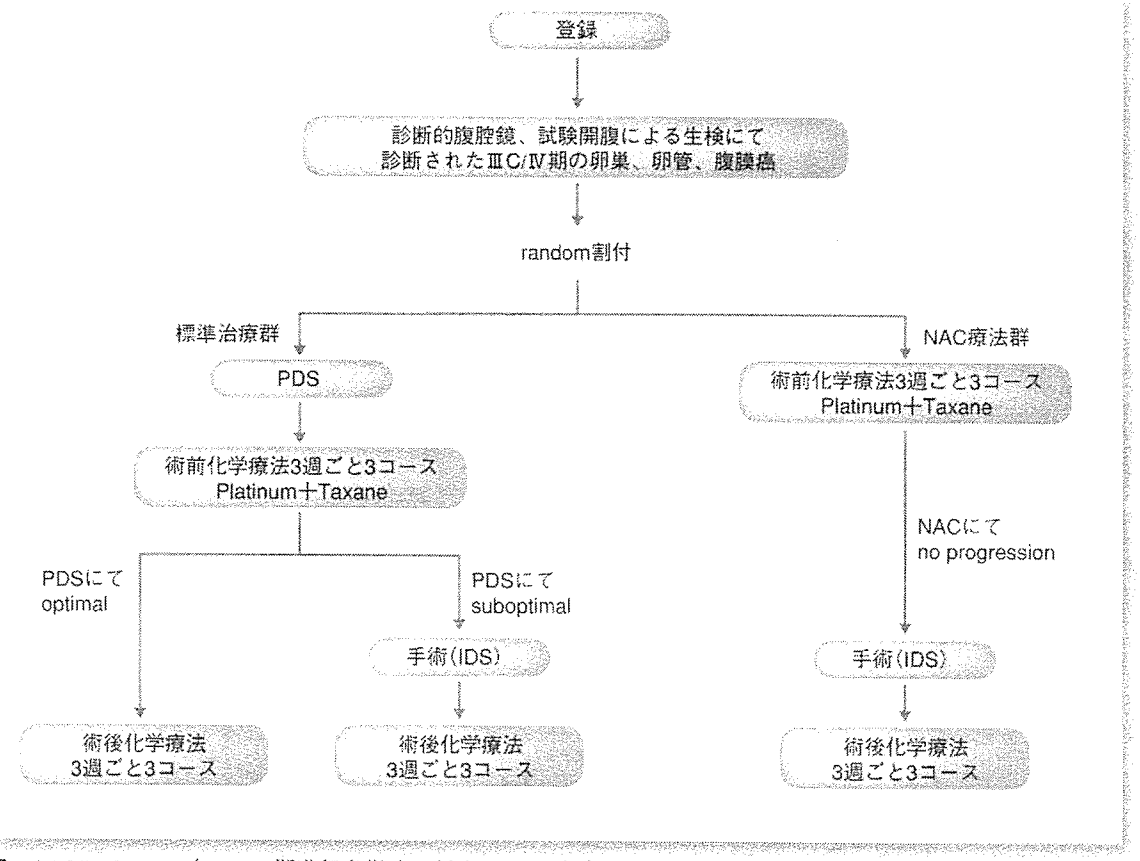

図1　EORTC55971（ⅢC/Ⅳ期進行卵巣癌に対するNAC療法と初回腫瘍縮小手術との第Ⅲ相ランダム化比較試験）

剤耐性細胞の出現数が多くなり、また血流不十分な細胞の存在により、薬剤耐性の出現の可能性も高くなる。

④腫瘍縮小手術に際して、肉眼的に腫瘍の縮小、消失が得られているため、術式を縮小しすぎて、かえって根治性を損なってしまう可能性がある。

②～④の問題点に関しては、これらの問題がありながらも、NAC療法が標準治療と同等あるいは優る治療成績が得られるのかを、NAC療法と標準治療のprospectiveな比較試験で検証する必要があると考えられる。

4. 進行中の臨床試験（prospective study）

Retrospective studyの結果を踏まえて、EORTC（European Organization for Research and Treatment of Cancer）のVergoteらは、第Ⅲ相ランダム化比較試験としてEORTC55971を行っている[12]（**図1**）。卵巣癌、卵管癌、腹膜癌のⅢC/Ⅳ期を対象に、診断的腹腔鏡、試験開腹、穿刺組織診のいずれかの方法で原発診断、組織診断、進行期診断の後、NAC療法群と手術先行の標準治療群にrandomizeしている。卵管癌、腹膜癌は、組織学的所見、化学療法感受性、予後が卵巣癌とほぼ同一であり、卵巣、卵管の摘出なしでは、鑑

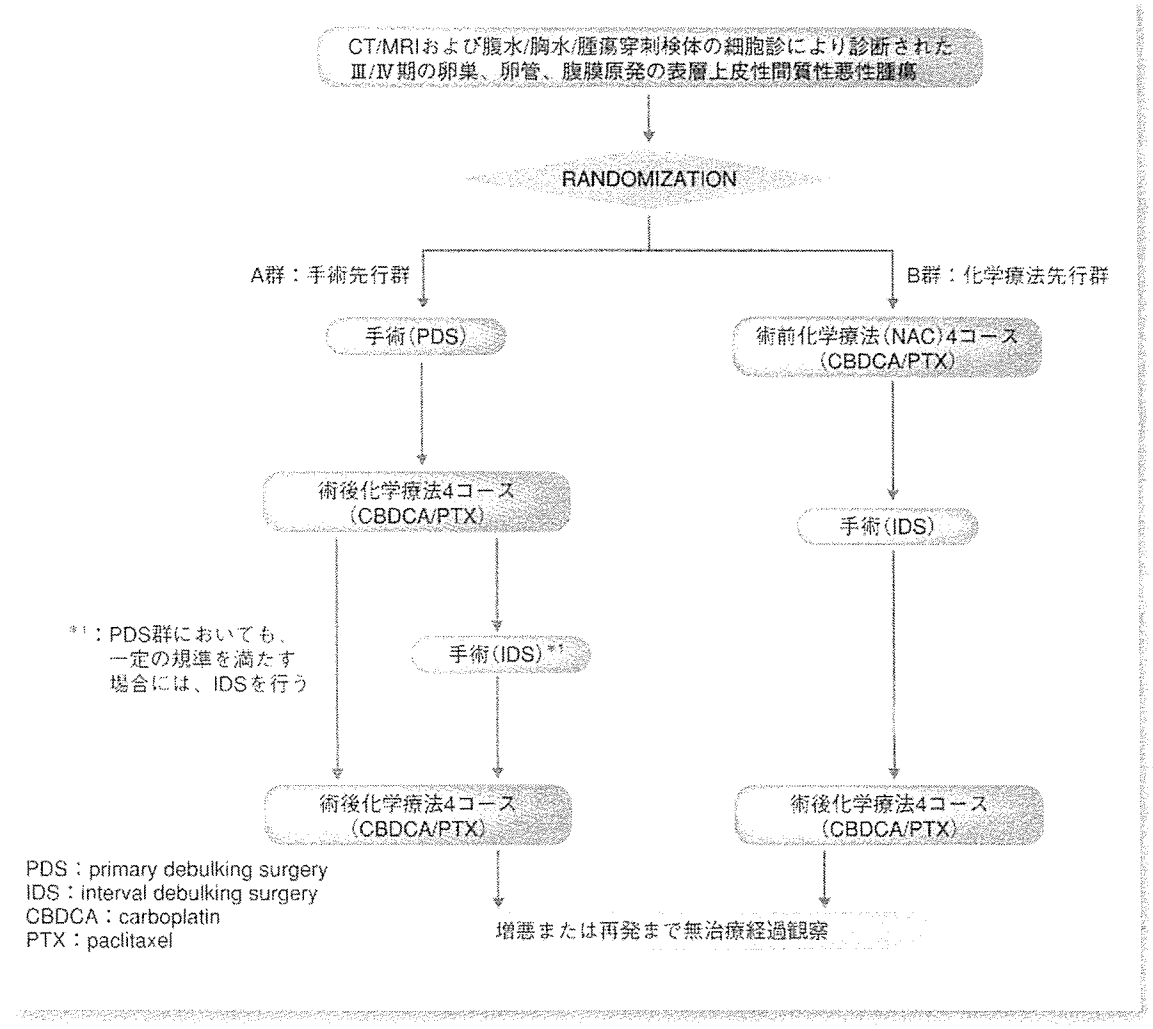

図2 JCOG0602(Ⅲ期/Ⅳ期卵巣癌、卵管癌、腹膜癌に対する手術先行治療 vs 化学療法先行治療のランダム化比較試験)

別診断困難であることから対象に含めている。プロトコール治療は、NAC療法群では、3コースの化学療法の後、腫瘍縮小手術(IDS)を行い、術後3コースの化学療法の追加、標準治療群ではPDSを行い、optimal surgeryが達成できた症例では、6コースの化学療法、suboptimalであった症例では、3コースの化学療法の後、腫瘍縮小手術(IDS)を行い、術後3コースの化学療法の追加である。多くの国から参加する試験のため、化学療法としては、参加施設の実状に合わせて、白金製剤(CDDP or CBDCA)＋タキサン系薬剤(PTX or DTX)のいずれの組み合わせでも可としている。この臨床試験は704例の登録予定で開始されたが、2006年10月時点でまだ登録中である。

JCOG(Japan Clinical Oncology Group)の婦人科腫瘍グループでも、同様の第Ⅲ相比較試験

(JCOG0602)を開始予定である。化学療法としては、日本で一般的に標準として用いられているPTXとCBDCAの組み合わせのTC療法で、術前(NAC)4コース、術後4コースのあわせて8コースを予定している(図2)。

これらの試験はいずれもNAC療法が標準治療に対して、効果の点で劣らないことを検証する非劣性試験である。NAC療法では手術に関連した侵襲の軽減(手術回数、輸血必要量など)が期待されるため、非劣性が証明されれば、NAC療法が進行卵巣癌の標準治療になると考えられる。

まとめ

卵巣癌に対するNAC療法は、その有用性に関して現在臨床試験が行われているところであり、いまだ結論は得られていない。Retrospective studyでの比較や、prospectiveな第Ⅱ相試験の結果からは、期待される治療ではあるが、現時点ではNAC療法はあくまでも試験的治療であり、臨床試験以外では治療開始時に手術を行うことが困難な全身状態の症例や、臨床的に腫瘍縮小手術不可能と判断される症例のみが対象となると考えられる。現在進行中の、prospectiveな第Ⅲ相比較試験により、NAC療法の有用性が確認され、今後進行卵巣癌の予後とQOLの改善が得られることに期待したい。

文献

1) Griffiths CT. Surgical resection of tumor bulk in the primary treatment of ovarian carcinoma. Natl Cancer Inst Monogr 1975; 42: 101-4.
2) Gershenson DM, McGuire WP, Gore M, Quinn MA, Thomas G. Controversies in Management. In: Gynecologic Cancer. Churchill Livingstone; 2004.
3) Bristow RE, Tomacruz RS, Armstrong DK, Trimble EL, Montz FJ. Survival effect of maximal cytoreductive surgery for advanced ovarian carcinoma during the platinum era: a meta-analysis. J Clin Oncol 2002; 20: 1248-59.
4) Covens AL. A critique of surgical cytoreduction in advanced ovarian cancer. Gynecol Oncol 2000; 78: 269-74.
5) Dauplat J, Le Bouedec G, Pomel C, Scherer C. Cytoreductive surgery for advanced stages of ovarian cancer. Semin Surg Oncol 2000; 19: 42-8.
6) FIGO (International Federation of Gynecology and Obstetrics) annual report on the results of treatment in gynecological cancer. Int J Gynaecol Obstet 2003; 83 Suppl 1: ix-xxii, 1-229.
7) Vergote I, De Wever I, Tjalma W, Van Gramberen M, Decloedt J, van Dam P. Neoadjuvant chemotherapy or primary debulking surgery in advanced ovarian carcinoma: a retrospective analysis of 285 patients. Gynecol Oncol 1998; 71: 431-6.
8) Kuhn W, Rutke S, Spathe K, Schmalfeldt B, Florack G, von Hundelshausen B, et al. Neoadjuvant chemotherapy followed by tumor debulking prolongs survival for patients with poor prognosis in International Federation of Gynecology and Obstetrics Stage Ⅲ C ovarian carcinoma. Cancer 2001; 92: 2585-91.
9) Ornis A, Marchetti M, Padovan P, Castellan L. Neoadjuvant chemotherapy in advanced ovarian cancer. Eur J Gynaecol Oncol 1996; 17: 393-6.
10) Kayikçioğlu F, Kose MF, Boran N, Caliskan E, Tulunay G. Neoadjuvant chemotherapy or primary surgery in advanced epithelial ovarian carcinoma. Int J Gynecol Cancer 2001; 11: 466-70.
11) Schwartz PE, Rutherford TJ, Chambers JT, Kohorn EI, Thiel RP. Neoadjuvant chemotherapy for advanced ovarian cancer: long-term survival. Gynecol Oncol 1999; 72: 93-9.
12) Vergote I, de Wever I, Tjalma W, Van Gramberen M, Decloedt J, Van Dam P. Interval debulking surgery: an alternative for primary surgical debulking? Semin Surg Oncol 2000; 19: 49-53.

Nuclear expression of S100A4 is associated with aggressive behavior of epithelial ovarian carcinoma: An important autocrine/paracrine factor in tumor progression

Norihiko Kikuchi, Akiko Horiuchi,[1] Ryosuke Osada, Tsutomu Imai, Cuiju Wang, Xiaojun Chen and Ikuo Konishi

Department of Obstetrics and Gynecology, Shinshu University School of Medicine, Nagano, Japan

(Received March 31, 2006/Revised June 30, 2006/Accepted July 3, 2006/Online publication August 28, 2006)

Although S100A4 expression has reportedly been associated with metastasis of various malignancies, little is known about its biological significance in ovarian carcinomas. In this study, we investigated expression and secretion of S100A4 and its extracellular function in ovarian carcinoma cells. We first used immunohistochemistry to examine the expression and localization of S100A4 in 113 epithelial ovarian neoplasms (24 benign, 20 borderline, and 69 malignant tumors) and analyzed its prognostic significance in patients with ovarian carcinoma. Then we investigated the expression, subcellular localization, and secretion of S100A4 in four ovarian carcinoma cell lines. Finally, we examined the effect of S100A4 treatment on the cell proliferation and invasiveness of ovarian carcinoma cells, along with activation of small GTPase, RhoA. Both cytoplasmic and nuclear expressions of S100A4 were significantly stronger in carcinomas than those in benign and borderline tumors. Ovarian carcinoma patients with strong nuclear S100A4 expression showed a significantly shorter survival than those without ($P = 0.0045$). This was not the case for cytoplasmic S100A4 expression. Ovarian carcinoma cell lines were shown to express S100A4, and secrete S100A4 into the culture media. Treatment with recombinant S100A4 resulted in the upregulation of S100A4 expression, translocation of S100A4 into the nucleus, and enhancement of invasiveness, which was associated with the upregulation of small GTPase, RhoA. These findings suggest that the nuclear expression of S100A4 is involved in the aggressive behavior of ovarian carcinoma and S100A4 is an autocrine/paracrine factor that plays an important role in the aggressiveness of ovarian carcinoma cells. (*Cancer Sci* 2006; 97: 1061–1069)

Epithelial ovarian carcinoma is the leading cause of death in female genital malignancies, and more than half of the patients are diagnosed at the advanced stage of disease.[1] The poor prognosis in patients with ovarian carcinoma is most likely related to the degree of peritoneal dissemination of cancer cells. The process of peritoneal dissemination is reportedly affected by a variety of gene products.[2–8] However, little is known about the molecular aspects of the migration and invasion of ovarian carcinoma cells. Recent attention has focused on the intracellular molecules involved in the enhancement of motility and invasiveness of cancer cells, and we previously showed that upregulation and activation of a small GTPase, RhoA, plays an important role in the tumor progression of ovarian carcinoma *in vivo* and *in vitro*.[9]

The S100A4 (also known as mts-1/metastasin/pEL98/p9ka) protein belongs to the S100 protein family, which consists of 21 small, acidic, calcium-binding proteins with two common EF-hand structure motifs.[10] S100A4 has been identified so far as a cytoplasmic protein that cosediments with cytoskeletal proteins such as actin, non-muscle myosin, and non-muscle tropomyosin, implying a possible role in cell motility and invasion.[11] Its relevance to the invasive or metastatic phenotype of cancer cells was shown by data from gene transfection,[12] and from transgenic animals.[13] S100A4 protein might also have functions in cell cycle progression.[14] Increased expression of S100A4 protein has been reported in various human cancers.[15] Interestingly, it has also been reported that some cells secrete S100 protein which might have extracellular functions, that is, extracellular S100A4 was reported to induce the outgrowth of hippocampal neurons,[16] or stimulate the capillary formation of endothelial cells.[17] Furthermore, a number of S100 proteins have been reported to translocate between the cytoplasm and the nucleus,[18] although their nuclear function is largely unknown.

In human epithelial ovarian neoplasms, however, there have been no available data on the expression and subcellular localization of S100A4. Secretion of S100A4 and its extracellular function have not been analyzed in ovarian carcinoma cells. In the present study therefore we examined the expression and localization of S100A4 in various epithelial ovarian tumors using immunohistochemistry, its subcellular localization by Western blotting, and analyzed its prognostic significance in patients with ovarian carcinoma. Then, we investigated the expression, subcellular localization, and secretion of S100A4 in ovarian carcinoma cells *in vitro*. Finally, we examined the effect of S100A4 treatment on the cell proliferation and invasiveness of ovarian carcinoma cells, along with activation of small GTPase, RhoA.

Materials and Methods

Patients and tissue samples. A total of 113 primary epithelial ovarian tumors were examined for immunohistochemistry. Sixty-nine patients with ovarian carcinoma visited Shinshu University Hospital (Nagano, Japan) between 1993 and 1999, and underwent surgery followed by cisplatin-based chemotherapy. The follow-up period ranged from 5 to 114 months (median: 47.3 months). According to the classification of FIGO, 33 carcinomas were classified as stage I, 10 were stage II, 21 were stage III, and 5 were stage IV. Histologically, 25 were serous, 5 mucinous, 22 clear cell and 17 endometrioid adenocarcinomas. With regard to histological grade,[19] 31 were graded as G1, 27 were G2, and 11 were G3. In 24 of the 69 cases, the specimens of peritoneal dissemination were available and also examined for immunohistochemistry. In addition, 24 cases of benign cystadenomas (4 serous, 20 mucinous) and 20 cases of borderline malignant tumors (8 serous, 12 mucinous) were selected from the pathology file of Shinshu University

[1]To whom correspondence should be addressed.
E-mail: aki9hori@hsp.md.shinshu-u.ac.jp
Abbreviations: FIGO, International Federation of Gynecology and Obstetrics; GAPDH, glyceraldehyde-3-phosphate dehydrogenase; GTP, guanosine triphosphate; OSE, ovarian surface epithelial; RT-PCR, reverse transcription-polymerase chain reaction.

doi: 10.1111/j.1349-7006.2006.00295.x

Hospital. Specimens were reviewed to confirm the histopathological diagnosis using the standard criteria.[20] These specimens were fixed in 10% phosphate-buffered formalin and embedded in paraffin. Serial sections of 3 μm thickness were made for hematoxylin–eosin staining and immunohistochemistry. Some of the fresh tissue blocks from the excised ovarian carcinoma were stored at −80°C for Western blotting. Each tissue sample was used with the approval of the Ethics Committee of Shinshu University School of Medicine.

Immunohistochemical analysis. Immunohistochemical staining was carried out by the streptavidin–biotin–peroxidase complex method using a Histofine SAB-PO kit (Nichirei, Tokyo, Japan). Three micrometer-thick sections were deparaffinized and boiled in 0.01 M citrate buffer (pH 6.0) for 25 min in a microwave oven. They were then treated with 0.3% hydrogen peroxide and incubated with 10% normal mouse serum. The sections were incubated with an anti-S100A4 rabbit polyclonal antibody (Dako, Glostrup, Denmark), which was used at a dilution of 1 : 50, at 4°C overnight. After washing in phosphate-buffered saline, they were incubated with biotinylated goat antirabbit immunoglobulin G, followed by treatment with peroxidase-conjugated streptavidin and stained with diaminobenzidine and 0.15% hydrogen peroxidase. Counterstaining was done with hematoxylin. Immunoreactive tumor cells were semiquantitatively estimated. Cytoplasmic staining was classified as: (–) negative, 0–10% positive cells; (+) weakly positive, 10–50% positive cells; and (+ +) strongly positive, more than 50% positive cells, by comparison with the positive internal control, that is, lymphocytes and vascular smooth muscle cells were positive for S100A4 in the cytoplasm.[21,22] Nuclear staining was defined as: (–) negative, 0–5% positive cells; (+) weakly positive, 5–20% positive cells; and (+ +) strongly positive, more than 20% positive cells. The evaluation of immunostaining was carried out by two independent observers (N.K. and A.H.) unaware of the fate of the patient or the tissue site.

Survival analysis. The log-rank test and Cox proportional hazards model were used to evaluate significant predictors of survival. The prognostic factors used in the survival analysis were as follows; FIGO stage, histological grade, results of S100A4 immunostaining. The log–rank test and Cox's univariate analysis were first carried out on each of the factors (PHREG procedure). Overall survival was then analyzed by the stepwise regression model using variables that showed significance by univariate analysis. Cumulative survival was also analyzed by the Kaplan–Meier method. Differences were considered to be significant at $P < 0.05$.

Preparation of nuclear and cytoplasmic protein fractions. Frozen ovarian carcinoma tissues were homogenized by a tissue homogenizer. Subfractioning of cell components was done using NE-PER Nuclear and Cytoplasmic Extraction Reagents (Pierce Biotechnology, Rockford, IL) according to the manufacturer's protocol.

Cell culture. The ovarian cancer cell lines SKOV3 and OVCAR3 were purchased from the American Type Culture Collection (Rockville, MD). The ovarian cancer cell lines A2780 and A2780/CDDP (a cisplatin-resistant cell line derived from A2780) were kind gifts from Dr Takashi Tsuruo (Cancer Chemotherapy Center, Tokyo, Japan),[23] with the permission of Dr Thomas C. Hamilton (Fox Chase Cancer Institute, Philadelphia, PA). A2780, A2780/CDDP, and OVCAR3 were maintained in RPMI-1640 (Sigma, St. Louis, MO) supplemented with 10% fetal bovine serum (Biomeda, Foster City, CA). SKOV3 was cultured in Dulbecco's modified Eagle's medium (Sigma) with 10% fetal bovine serum. Incubation was carried out at 37°C under 5% CO_2 in air.

OSE cells were obtained from three women who were treated surgically for benign gynecologic disease, after obtaining written consent from each patient. Cell culture was carried out as described previously.[3]

Treatment with recombinant S100A4. Human recombinant S100A4 protein was produced from human cDNA and kindly provided by Dr C.W. Heizmann (Division of Clinical Chemistry, Department of Pediatrics, University of Zurich, Switzerland). Recombinant A100A4 was added to the serum-free culture media at a concentration of 10^{-14}, 10^{-12} and 10^{-10} M.

Immunofluorescence staining. Cultured cells in a two-well Laboratory-Tek Chamber Slide were fixed in cold acetone for 15 min, then 0.3% hydrogen peroxide was applied to block endogenous peroxide activity, and the cells were incubated with normal mouse serum. The cells were incubated with an anti-S100A4 antibody at room temperature for 1 h, and fluorescein-isothiocyanate-labeled goat antirabbit immunoglobulin G was used. Propidium iodide (Calbiochem, San Diego, CA) was used to stain DNA. All specimens were examined using a Laser Scanning Spectral Confocal Microscope (Leica TCS SP2; Leica Microsystems, Wetzlar, Germany).

Immunoprecipitation for secreted S100A4. The S100A4 secretion was examined using a Protein A Immunoprecipitation Kit (Kirkegaard & Perry Laboratories, Gaithersburg, MD). After cells were cultured for 24 h, 1 mL of culture medium was collected and incubated with 1 μg of anti-S100A4 antibody overnight. Protein A agarose was added and the mixture was incubated at room temparature for 1 h. After heating the sample at 95°C for 2 min, it was centrifuged at 13 000*g* for 20 min at 4°C and the supernatants were stored at −80°C.

Western blot analysis. Extracts equivalent to 30 μg of total protein were separated by sodium dodecylsulfate–polyacrylamide gel electrophoresis (12% acrylamide) and transferred onto nitrocellulose membranes (Hybond-C super; Amersham Biosciences, Piscataway, NJ) as described previously.[9] The first antibodies against S100A4, RhoA (Santa Cruz Biotechnology, Santa Cruz, CA), MT1-MMP (Sigma) or β-actin (BioMakor, Rehovot, Israel) were used.

RT-PCR. Total RNA was extracted by the acid guanidinium–phenol–chloroform method.[24] One microgram of total RNA was treated with 1 U/10 μL DNase I (Life Technologies, Gaithersburg, MD). RT-PCR was carried out using an RNA PCR Kit (Takara Shuzo, Otsu, Japan) as described previously.[3,9] Primers were synthesized to encompass a specific segment of the cDNA sequence of the S100A4 (sense, 5′-agcttcttggggaaaaggac-3′ and antisense, 5′-ccccaaccacatcagagg-3′), RhoA (sense, 5′-ctggtgattgttggtgatgg-3′ and antisense, 5′-gcgatcataatcttcctgcc-3′), or of GAPDH (sense, 5′-acgaccactttgtcaagctc-3′ and antisense, 5′-ggtctacatggcaactgtga-3′). The corresponding cDNA fragments were denatured at 94°C for 30 s, annealed at 58°C for 1 min, and extended at 72°C for 1 min. After 35 cycles of amplification, the PCR products were analyzed on a 2% agarose gel, and the bands were visualized using ethidium bromide.

Cell proliferation assay. Cell number and viability were further assessed by using the reagent WST-1 (Roche, Indianapolis, IN). Cells under different treatments ($n = 32$ of each group) were plated at 1×10^4 cells/0.32 cm^2 in a 96-well plate and maintained for 48 h at 37°C with 5% CO_2. This was followed by incubation with WST-1 reagent for 4 h. After thorough shaking, each sample was measured at a wavelength of 450 nm with Multiscan JX (Thermo Labsystems, Vantee, Finland). Absorbance readings were normalized against control wells with medium alone.

***In vitro* invasion assay.** Cell invasion through a reconstituted basement membrane (Matrigel; BD Biosciences, Bedford, MA), was assayed by a method reported previously.[9,25] After 22 h of incubation under different treatments, serum-free medium with 0.1% bovine serum albumin as control, recombinant S100A4, cultured medium of A2780/CDDP, C3 exoenzyme (Alexis Biochemicals, Lausen, Switzerland) and Y27632 (Calbiochem), the invaded cells were counted in 10 different fields under a light microscope at ×400 magnification. Each experiment was done in triplicate wells and repeated three times.

Migration assay. Cell migration was examined using a monolayer wounding system as previously described.[26]

doi: 10.1111/j.1349-7006.2006.00295.x

Rho-GTP pull-down assay. The Rho-GTP pull-down assay was carried out using a Rho Activation Assay Biochem Kit (Cytoskeleton, Denver, CO). In brief, all cells were washed with ice-cold phosphate-buffered saline and lyzed with lysis buffer. After being centrifuged at 8500 *g* for 5 min, Rhotekin (Rho effector)–Rho binding domain protein, which has high affinity for activated GTP-Rho, bound to glutathione–agarose was added to the cell lysate and incubated for 1 h at 4°C on a rocker. After centrifugation, Rho-GTP bound to beads was washed with lysis buffer and eluted in Laemmli sample buffer. Proteins were analyzed by Western blotting using antibodies against RhoA.

Statistical analyses. Statistical analysis was carried out with the Kruskal–Wallis rank test, Scheffe and Mann–Whitney's *U*-test were used to compare the expression in immunohistochemistry.

Results

Expression of S100A4 in the cytoplasm and nuclei is increased in ovarian carcinomas compared with benign/borderline tumors. Representative profiles of immunostaining for S100A4 are shown in Figure 1. Specific staining for S100A4 was commonly observed in the cytoplasm. However, in some cases, both cytoplasmic and nuclear staining were observed. Correlations between S100A4 immunostaining and clinicopathological findings are summarized in Tables 1 and 2.

The cytoplasmic S100A4 expression was significantly stronger in ovarian carcinomas than in benign ($P < 0.0001$) and borderline tumors ($P = 0.0288$). According to the FIGO stage classification, although the number of cases strongly positive for cytoplasmic expression was higher in stage III/IV (88%) than in stage I/II (65%) ($P = 0.0672$), there was no significant difference. The cytoplasmic expression of S100A4 in the metastatic lesion was compared to the respective primary lesion in 24 cases; it was increased or similar in 18 (75%) cases, and decreased in the remaining six cases.

Nuclear immunostaining strongly positive for S100A4 was observed in none of the 24 benign cystadenomas, 3 (15%) of the 20 borderline tumors, and 17 (25%) of the 69 ovarian carcinomas (Fig. 1c,d and Table 2). The rate of nuclear strong positivity was significantly higher in carcinoma than in benign ($P < 0.0001$) and borderline tumors ($P = 0.0154$). There was no significant difference according to the histological type, the FIGO stage or histological grade. The nuclear expression of S100A4 in the metastatic lesion was compared to the respective primary lesion in 24 cases; it was increased or similar in 14 (58%) cases, and decreased in the remaining 10 cases.

Elevated expression of S100A4 in the nuclei is correlated with poor prognosis of ovarian carcinoma patients. All 20 patients with borderline tumors were alive with no evidence of recurrence at the last follow-up. Of the 69 patients with ovarian carcinoma, 25 had died of disease. Of the remaining 44 patients, 43 were alive and one had died of another disease. The prognosis was significantly poorer in patients with advanced FIGO stages (overall survival: stage I + II, 58.4 ± 27.1 months *versus* stage III + IV, 22.8 ± 22.6 months, $P < 0.0001$), in patients with high grade (G1, 52.3 ± 28.1 months *versus* G2 + G3, 43.1 ± 29.7 months, $P = 0.0218$). In patients of all stages, the prognosis was

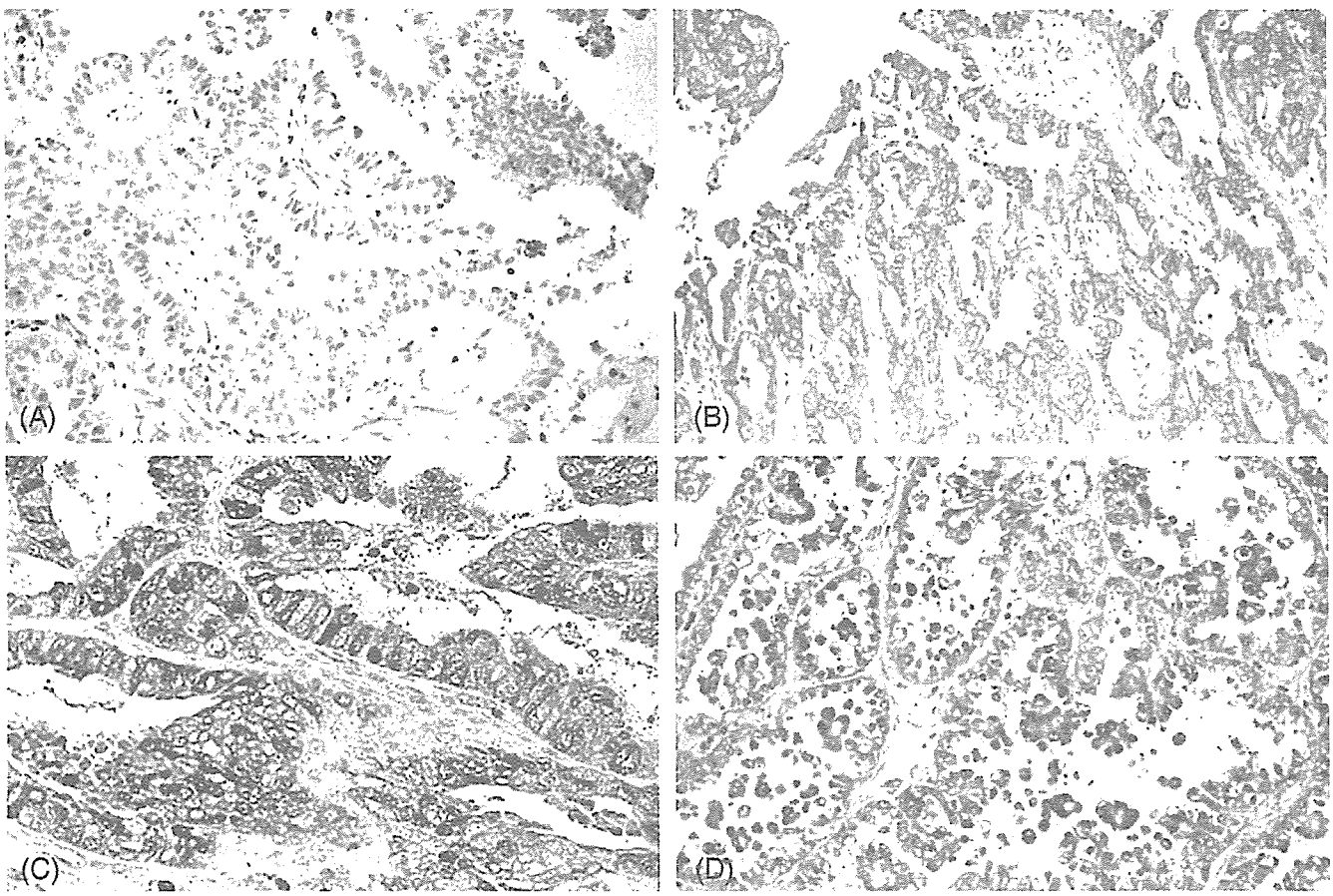

Fig. 1. Immunohistochemical staining of S100A4 in various epithelial ovarian tumors. (A) Serous borderline tumor negative for S100A4 expression. (B) Serous carcinoma showing S100A4 positivity in the cytoplasm. (C) Endometrioid carcinoma showing S100A4 positivity both in the cytoplasm and in the nucleus. (D) Clear cell carcinoma showing S100A4 positivity both in the cytoplasm and in the nucleus (magnification: ×100).

Table 1. Immunohistochemical cytoplasmic expression of S100A4 in epithelial ovarian neoplasms

	Total number of cases	Cytoplasmic staining		
		–	+	+ +
Benign cystadenomas	24	19 (79%)	1 (4%)	4 (17%)
Serous	4	0	1	3
Mucinous	20	19	0	1
Borderline tumors	20	8 (40%)	1 (5%)	11 (55%)
Serous	8	3	0	5
Mucinous	12	5	1	6
Carcinomas	69	5 (7%)	13 (19%)	51 (74%)
FIGO stage				
I	33	4	7	22
II	10	1	3	6
III	21	0	1	20
IV	5	0	2	3
Histological type				
Serous	25	0	3	22
Mucinous	5	0	1	4
Endometrioid	17	3	4	10
Clear cell	22	2	5	15
Histological grade				
G1	31	2	3	26
G2	27	2	9	16
G3	11	1	1	9

–, 0–10% positive cells; +, 10–50% positive cells; + +, more than 50% positive cells.

Table 2. Immunohistochemical nuclear expression of S100A4 in epithelial ovarian neoplasms

	Total number of cases	Nuclear staining		
		–	+	+ +
Benign cystadenomas	24	24 (100%)	0 (0%)	0 (0%)
Serous	4	4	0	0
Mucinous	20	20	0	0
Borderline tumors	20	17 (85%)	0 (0%)	3 (15%)
Serous	8	6	0	2
Mucinous	12	11	0	1
Carcinomas	69	34 (49%)	18 (26%)	17 (25%)
FIGO stage				
I	33	20	8	5
II	10	5	2	3
III	21	6	8	7
IV	5	3	0	2
Histological type				
Serous	25	11	6	8
Mucinous	5	1	3	1
Endometrioid	17	9	4	4
Clear cell	22	13	5	4
Histological grade				
G1	31	17	7	7
G2	27	13	8	6
G3	11	4	3	4

–, 0–10% positive cells; +, 10–20% positive cells; + +, more than 20% positive cells.

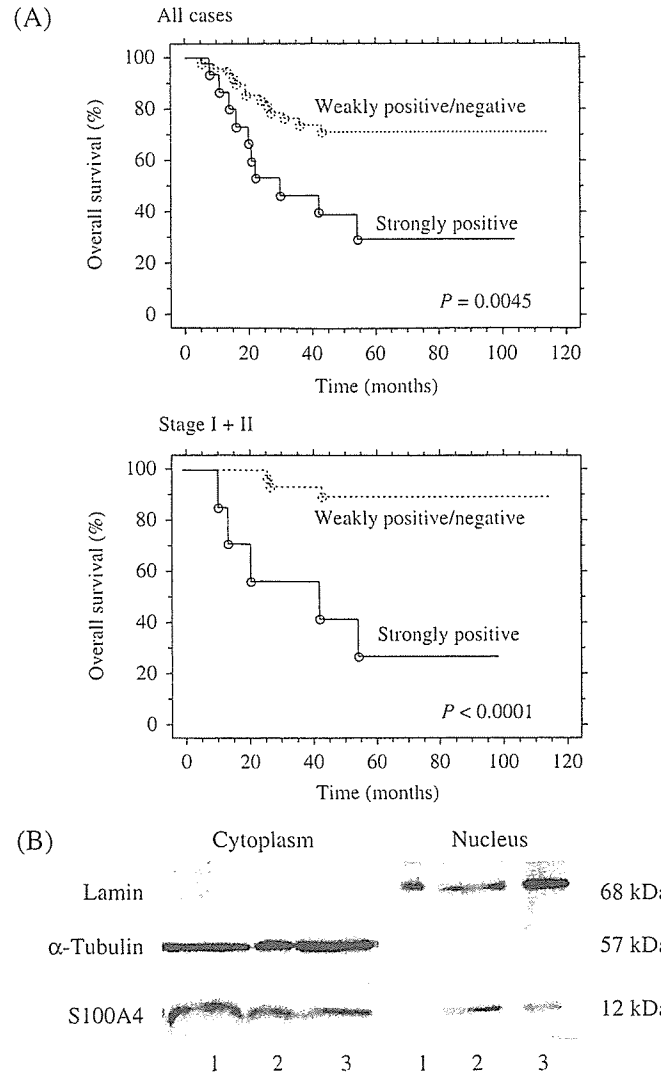

Fig. 2. (A) Overall survival of ovarian carcinoma patients according to the nuclear S100A4 expression. Kaplan–Meier analysis shows significantly poorer survival in patients with strong nuclear S100A4 expression compared to those with weakly positive/negative nuclear S100A4 expression. (B) Western blot analysis of cytoplasmic and nuclear fractions obtained from three carcinoma tissues. Lane 1, serous carcinoma shown in Figure 1b; lane 2, endometrioid carcinoma shown in Figure 1C; lane 3, clear cell carcinoma shown in Figure 1D. The presence of S100A4 not only in the cytoplasmic but also in the nuclear fraction was observed in both cases (lanes 2 and 3) that showed nuclear staining of S100A4 (Fig. 1C,D). Lamin B and α-tubulin were used as the markers for nuclear and cytoplasmic fractions, respectively.

significantly poorer in patients with strong nuclear expression of S100A4 (strongly positive, 39.1 ± 30.1 months *versus* weakly positive/negative, 49.8 ± 28.7 months, $P = 0.0045$) (Fig. 2a). This was not the case for cytoplasmic S100A4 expression. Interestingly, among the patients with FIGO stage I + II, the prognosis was significantly poorer in those with strong nuclear positivity for S100A4 (strongly positive, 43.1 ± 31.2 months *versus* weakly positive/negative, 61.6 ± 25.5 months, $P < 0.0001$) (Fig. 2A), but was not statistically significant in those with stage III + IV (strongly positive, 35.6 ± 30.7 months *versus* weakly positive/negative, 25.4 ± 17.5 months, $P = 0.7559$). Multivariate analysis in stage I + II cases also showed that strong nuclear expression of S100A4 was an independent prognostic factor ($P = 0.0009$).

doi: 10.1111/j.1349-7006.2006.00295.x

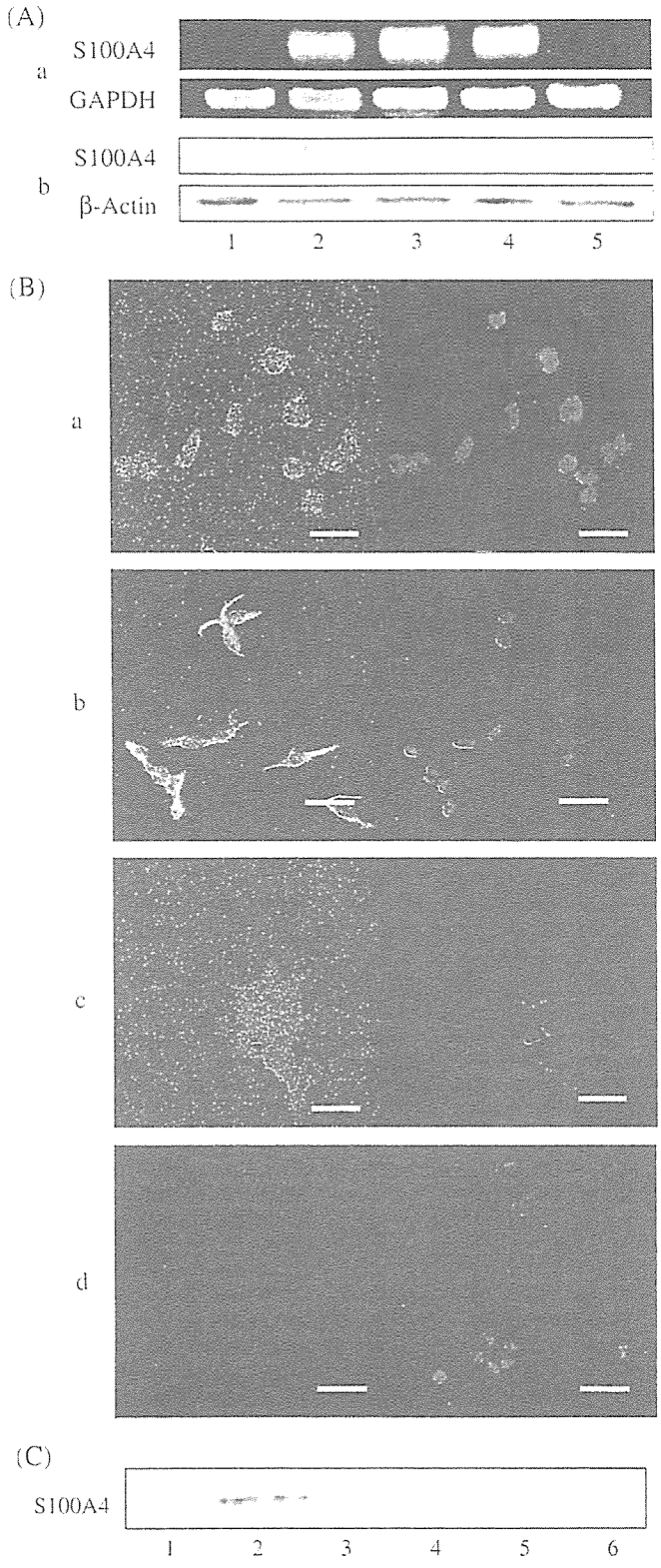

Fig. 3. (A) RT-PCR (a) and Western blot (b) analyses for the expression of S100A4 in normal OSE cells (1) and ovarian carcinoma cells (2, A2780; 3, A2780/CDDP; 4, SKOV3; 5, OVCAR3). S100A4 expressions at both mRNA and protein levels are observed in three ovarian carcinoma cells, but not in normal OSE or ovarian carcinoma OVCAR3 cells. (B) Immunofluorescent analysis for the subcellular localization of S100A4 in ovarian carcinoma cells. A2780 (a) and A2780/CDDP (b) cells show both cytoplasmic and nuclear expressions, whereas SKOV3 cells show only cytoplasmic expression (c) and OVCAR3 cells show faint cytoplasmic expression (d). Left panel, S100A4 staining; right panel, propidium iodide staining. Bar, 40 μm. (C) Western blot analysis for S100A4 in the culture media from ovarian carcinoma cells (lane 1, A2780; lane 2, A2780/CDDP; lane 3, OVCAR3; lane 4, SKOV3) and culture medium without cells (lane 5, RPMI-1640; lane 6, Dulbecco's modified Eagle's medium). Secretion of S100A4 into the culture media is confirmed in A2780, A2780/CDDP, and SKOV3 cells, but not in OVCAR3 cells.

To examine whether S100A4 protein is actually present in the nuclei of tumor cells, nuclear and cytoplasmic protein fractions were obtained from the three carcinoma cases, a serous carcinoma (Fig. 1B), an endometrioid carcinoma (Fig. 1C) and a clear cell carcinoma (Fig. 1D). In both cases that showed nuclear staining of S100A4 (Fig. 1C,D), the band for S100A4 was observed not only in the cytoplasmic compartment, but also in the nuclear compartment (Fig. 2B). These results confirmed that S100A4 protein existed in the nuclei of carcinoma cells.

S100A4 is expressed in ovarian carcinoma cells, localized either in the cytoplasm or in the nuclei, and secreted into culture media. Expression of S100A4 in the four ovarian carcinoma cell lines and normal OSE cells at the mRNA and protein levels was investigated with RT-PCR and Western blot. RT-PCR showed that an intense band observed at 200 bp for S100A4 was also observed in three (A2780, A2780/CDDP and SKOV3) of four ovarian carcinoma cells (Fig. 3A: a, lanes 2–4). In contrast, a band for S100A4 was not obtained in normal OSE cells (Fig. 3A: a, lane 1) or in OVCAR3 cells (Fig. 3A: a, lane 5). Western blot analysis revealed an intense band at 12 kDa for S100A4 was evident in three of four ovarian carcinoma cell lines (Fig. 3A: b, lanes 2–4). The specific band was not observed in normal OSE (Fig. 3A: b, lane 1) or OVCAR3 cells (Fig. 3A: b, lane 5), whereas the 42 kDa band for β-actin was observed in all of the cell samples. Thus, the expression of S100A4 at mRNA and protein levels was shown in ovarian carcinoma cells such as A2780, A2780/CDDP and SKOV3, except for OVCAR3. In contrast, normal OSE cells did not express S100A4.

Immunofluorescent analysis showed that specific staining for S100A4 was identified as a green signal in the nucleus and/or cytoplasm. In A2780 and A2780/CDDP cells, diffuse staining of S100A4 both in the cytoplasm and in the nucleus was observed (Fig. 3B: a,b). In SKOV3 cells, diffuse staining of S100A4 was observed only in the cytoplasm (Fig. 3B: c). In contrast, the expression of S100A4 was faint in OVCAR3 cells (Fig. 3B: d). These results were consistent with our data from Western blotting.

The existence of S100A4 in cultured media was investigated. Specific 12 kDa bands for S100A4 were detected in the cultured media from A2780, A2780/CDDP and SKOV3 (Fig. 3C, lanes 1, 2 and 4), all of which expressed S100A4. In contrast, S100A4 was not detected in culture medium from OVCAR3 (Fig. 3C, lane 3). These results confirmed that S100A4-positive ovarian carcinoma cells secrete S100A4 protein into cultured medium.

S100A4 treatment induces upregulation of S100A4 along with its translocation into the nuclei. Next, we investigated the effect of extracellular S100A4 in ovarian carcinoma cells. In SKOV3 and OVCAR3, the intensity of the band for S100A4 mRNA was increased by treatment with recombinant S100A4 (Fig. 4A: a). The band for S100A4 protein was also increased by S100A4 treatment (Fig. 4A: b). Such an increase in the S100A4 expression at both the mRNA and protein levels occurred 2 h after addition of S100A4. The peak of the increase in the mRNA and protein expression was noted at 12 h after the S100A4 treatment (Fig. 4A: a,b).

We also analyzed the change in the subcellular localization of S100A4 in SKOV3 and OVCAR3 cells using immunofluorescence staining. Without addition of recombinant of S100A4, expression of S100A4 was observed only in cytoplasm in SKOV3

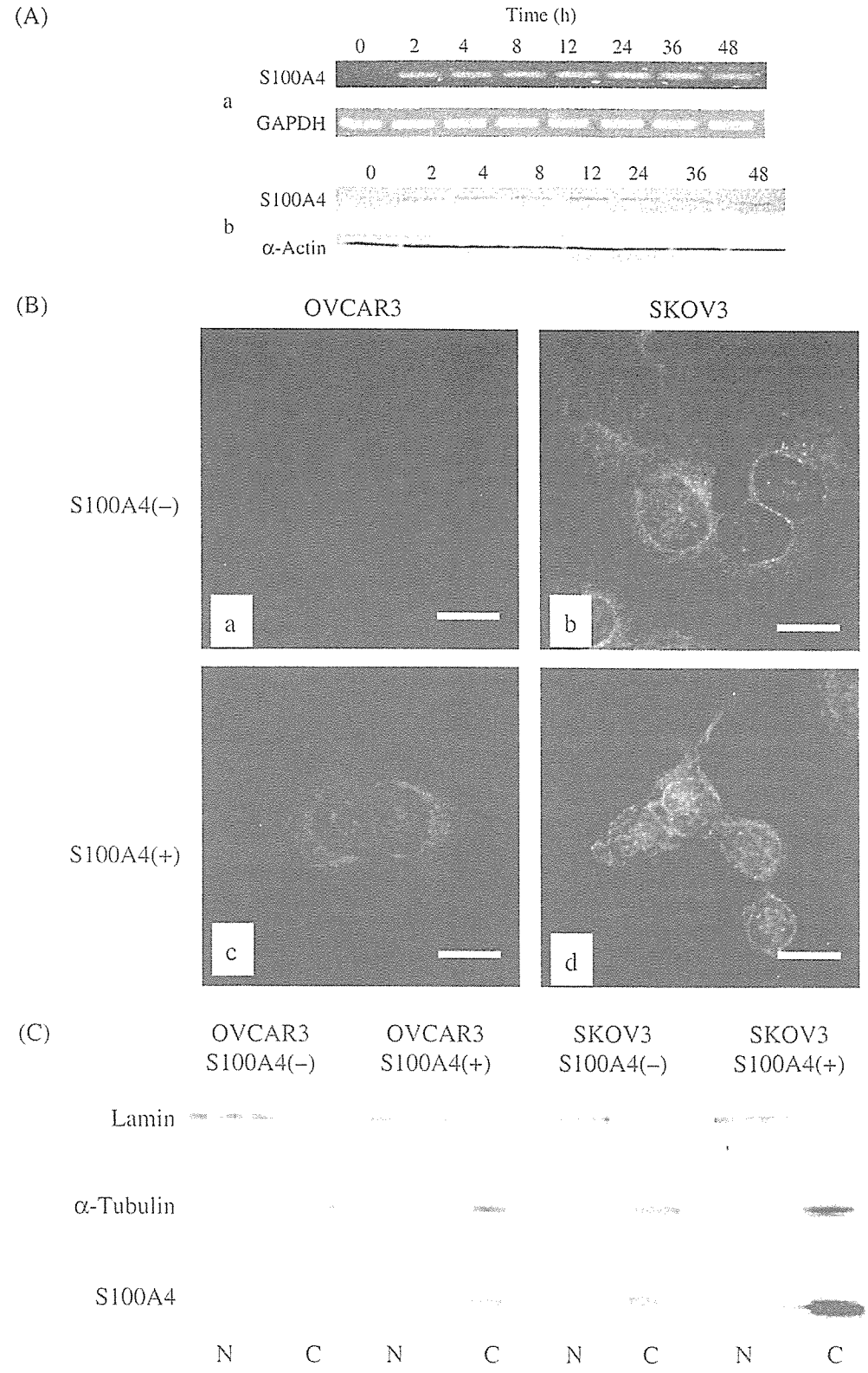

Fig. 4. (A) RT-PCR (a) and Western blot (b) analyses for the expression of S100A4 in ovarian carcinoma OVCAR3 cells after treatment with recombinant S100A4. Expression of S100A4 at both mRNA and protein levels occurred 2 h, and peaked at 12 h, after the treatment. (B) Immunofluorescent analysis for the subcellular localization of S100A4 showing SKOV3 cells (a) and OVCAR3 cells (b) without S100A4 treatment, and SKOV3 cells (c) and OVCAR3 cells (d) with S100A4 treatment. After the S100A4 treatment, nuclear expression of S100A4 appeared in SKOV3 cells (c), and cytoplasmic expression increased in OVCAR3 cells (d). Bar, 20 μm. (C) Western blot analysis of cytoplasmic and nuclear fractions showing the S100A4 treatment increased cytoplasmic expression in both SKOV3 and OVCAR3 cells. Moreover, the presence of S100A4 in the nuclear fraction was observed in SKOV3 cells after S100A4 treatment. C, cytoplasmic fractions; N, nuclear fractions.

doi: 10.1111/j.1349-7006.2006.00295.x

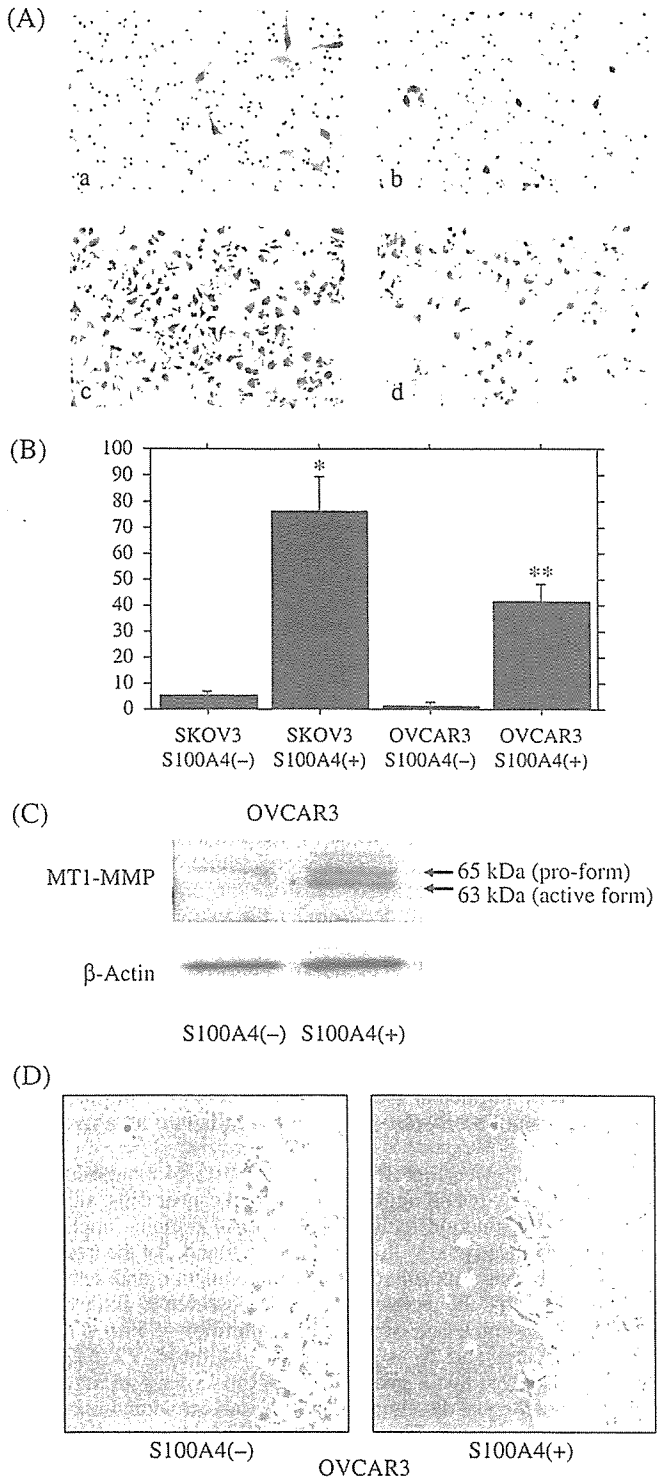

Fig. 5. (A) Matrigel invasion assay showing that treatment with recombinant S100A4 resulted in an increase in invasiveness in both SKOV3 cells and OVCAR3 cells. Microphotographs showing SKOV3 cells (a) and OVCAR3 cells (b) without S100A4 treatment, and SKOV3 cells (c) and OVCAR3 cells (d) with S100A4 treatment. (B) Count of invaded cells showing the significant increase in invasiveness after the S100A4 treatment. $*P < 0.0001$; $**P < 0.0001$. (C) Western blot analysis showing S100A4 treatment increased the active form of MT1-MMP in OVCAR3 cells. (D) Cells were incubated in serum-free RPMI-1640 with or without 10^{-10} M recombinant S100A4 for 22 h. Scratch wound assay showed that S100A4 treatment induced the migration of carcinoma cells along with the changes in cell shape.

cells (Fig. 4B: b), however, nuclear expression of S100A4 appeared after the addition of recombinant S100A4 (Fig. 4B: d), indicating the translocation of S100A4 from the cytoplasm into the nucleus. In OVCAR3 cells, although S100A4 treatment increased the cytoplasmic expression of S100A4, its nuclear expression was not observed (Fig. 4B: c). To confirm the subcellular expression pattern of S100A4, the nuclear and cytoplasmic protein fractions were obtained from SKOV3 with or without addition of recombinant S100A4. Western blotting revealed that cytoplasmic S100A4 expression was increased in both cell lines and the nuclear compartments were induced in SKOV3 cells after the S100A4 treatment (Fig. 4C).

S100A4 treatment does not alter the cell proliferation, but enhances the invasiveness of ovarian cancer cells along with upregulation and activation of RhoA. We then analyzed the effect of extracellular S100A4 on the cell proliferation and invasiveness in two ovarian cancer cell lines, SKOV3 and OVCAR3. A WST-1 assay revealed that treatment with recombinant S100A4 did not change the number of viable cells in either cell line (data not shown). A Matrigel invasion assay showed that treatment with recombinant S100A4 significantly stimulated the *in vitro* invasiveness in both cell lines in a dose-dependent manner (Fig. 5A,B). As the results from Matrigel invasion assay present the sum of proteolysis and migration, we further investigated MT1-MMP activity, according to a previous report,[27] and scratch assay. Western blot analysis for MT1-MMP revealed that the treatment with recombinant S100A4 increased the active form of MT1-MMP (Fig. 5C) in OVCAR3 cells. In addition, migration of OVCAR3 cells was also stimulated by treatment with recombinant S100A4 (Fig. 5D). Treatment with conditioned media from A2780/CDDP, which actively secrete S100A4, also enhanced the invasiveness of SKOV3 and OVCAR3 cells (Fig. 6).

Finally, we investigated the role of small GTPase, RhoA, in the S100A4-induced increase in invasiveness. The expression of RhoA at the mRNA and protein levels was increased by treatment with recombinant S100A4 (Fig. 6A: a,b). The peaks of their expressions were noted at 12 h after treatment, just after the peak of S100A4 expression. In addition, a Rho-GTP pull-down assay revealed that S100A4 treatment increased the amount of the GTP-binding form of RhoA, that is, activation of RhoA occurred (Fig. 6B). To confirm the involvement of the Rho pathway in the stimulation of invasion under extracellular S100A4, we used C3 exoenzyme (a specific inhibitor of Rho) and Y27632 (Rho kinase inhibitor). When the SKOV3 cells were treated with C3 exoenzyme or A27632 for 22 h, the S100A4-induced enhancement of cell invasion was completely suppressed (Fig. 6C).

Discussion

The present study showed that, among various epithelial ovarian neoplasms, the cytoplasmic and nuclear expressions of S100A4 obtained by immunohistochemistry were significantly stronger in invasive carcinomas than in benign cystadenomas. More interestingly, strong expression of S100A4 in the nucleus was an independent prognostic factor in patients with ovarian carcinoma. Kaplan–Meier analysis showed that patients with strong nuclear staining of S100A4 had a significantly shorter survival period compared to those without, especially in stage I/II disease. The preparation of cytoplasmic and nuclear fractions followed by Western blot analysis confirmed the presence of nuclear S100A4 protein in ovarian carcinoma tissues with nuclear immunostaining. Although the prognostic impact of cytoplasmic expression of S100A4 was reported in breast[28] and gastric carcinoma,[29] this is the first report showing the importance of nuclear S100A4 in the patient prognosis. Little is known about the prognostic indicators other than histological grade for early stage ovarian carcinomas, in which fertility-sparing surgery is sometimes needed. Thus,

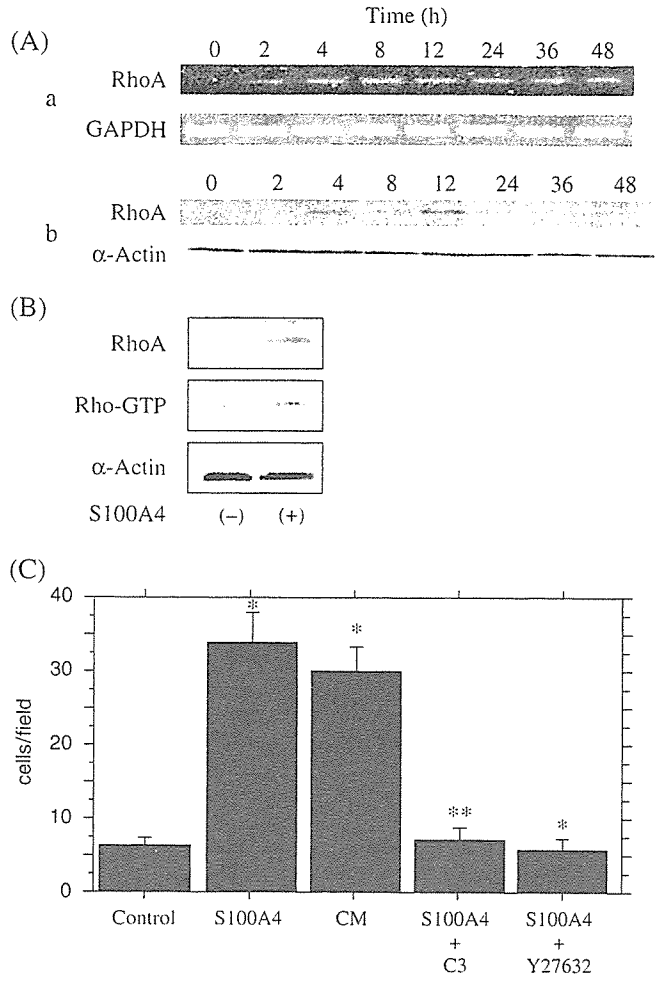

Fig. 6. (A) RT-PCR (a) and Western blot (b) analyses for the expression of RhoA in ovarian carcinoma OVCAR3 cells after the S100A4 treatment. Expression of RhoA is increased at both mRNA and protein levels after the S100A4 treatment. (B) Rho-GTP pull-down assay showing that the activated form of RhoA is increased after S100A4 treatment. (C) Matrigel invasion assay showing that invasiveness of OVCAR3 cells is also increased by treatment with conditioned media (CM) from A2780/CDDP containing S100A4. Increase in invasiveness by treatment with S100A4 or A2780/CDDP-conditioned media is suppressed by simultaneous treatment with Rho inhibitors such as C3 exoenzyme and Y27632. $*P < 0.0001$; $**P < 0.0001$.

development of a novel marker indicating aggressiveness in patients with early stage disease is needed in clinical practice. Further collection of such early stage ovarian carcinoma cases is needed to establish the prognostic significance of nuclear S100A4 expression.

Based on the *in vivo* data on S100A4 expression in ovarian carcinomas, we hypothesized that it plays an important role in the aggressive characteristics in ovarian carcinomas. To address this hypothesis, we tested *in vitro* S100A4 expression, secretion, and nuclear translocation, and its functional relevance to cell proliferation and invasiveness using four ovarian carcinoma cell lines, A2780, A2780/CDDP, SKOV3, and OVCAR3. RT-PCR and Western blot analysis showed that ovarian carcinoma cells express S100A4 at the mRNA and protein levels, except for OVCAR3. Immunofluorescent analysis showed that nuclear localization of S100A4 was observed in A2780 and A2780/CDDP, but not in SKOV3. Interestingly, the difference in the expression and subcellular localization of S100A4 among the four cell lines paralleled the difference in aggressiveness in a nude mouse model of peritoneal dissemination; A2780 and A2780/CDDP were aggressive, SKOV3 was intermediate, and OVCAR3 was the least aggressive (A. Horiuchi *et al*, unpublished data, 2004). In addition, immunoprecipitation analysis showed that all of the cell lines except for OVCAR3 secreted S100A4 protein into the culture media. Furthermore, all four cell lines expressed the mRNA and protein of RAGE, the receptor for S100 family proteins (N. Kikuchi *et al*, unpublished data, 2004). These findings suggest that S100A4 can act as an autocrine/paracrine factor in ovarian carcinoma cells. Therefore, we used recombinant S100A4 in our experiments in order to analyze the effect of extracellular S100A4 on ovarian carcinoma cells.

Our study showed that treatment with recombinant S100A4 did not alter cell proliferation, but significantly enhanced the *in vitro* invasiveness of ovarian carcinoma cells, SKOV3 and OVCAR3, in a dose-dependent manner. Interestingly, along with the increase in invasive capacity, S100A4 treatment induced evident expression of S100A4 in the cytoplasm in OVCAR3 cells, and also upregulated the S100A4 expression in SKOV3 cells, suggesting the presence of a positive feedback mechanism for the S100A4 expression in ovarian carcinoma cells. In addition, our immunofluorescent analysis showed that S100A4 treatment resulted in the translocation of S100A4 from the cytoplasm into the nucleus in SKOV3 cells. Although S100A4 was first identified as cytoplasmic protein, its translocation between the cytoplasm and the nucleus has been reported in human cells *in vitro*, such as endothelial cells,[30] fibroblasts,[31] glioblastoma cells,[32] and colorectal carcinoma.[33] S100A4 has been implicated in the regulation of gene transcription either through direct DNA binding, or through interaction with other DNA-binding proteins.[33] S100 family proteins are calcium-binding proteins with two common EF-hand structure motifs, and their change in the intracellular localization was shown to be dependent on the intracellular concentration of calcium.[18,34] The intracellular translocation of an S100 protein has also been reported to occur under the extracellular presence of the same S100 protein.[30] However, the question remains how S100A4 translocates between cytoplasm and nucleus in ovarian cancer cells. In ovarian carcinoma SKOV3 cells, nuclear translocation of S100A4 along with enhanced invasiveness was induced by extracellular S100A4. Nuclear expression of S100A4 was correlated with poor prognosis in ovarian carcinomas. All these data suggest that nuclear localization of S100A4 is important in the transformation of ovarian carcinoma cells into an aggressive phenotype.

Our study showed that treatment with S100A4 increased both MT1-MMP activity and migration in ovarian cancer cells, although the signal transduction pathway of S100A4 remains unclear in the enhanced invasiveness. In this study, we found that the treatment with recombinant S100A4 resulted in upregulation and activation of RhoA, and that the increase in invasiveness due to extracellular S100A4 was suppressed by a specific inhibitor of Rho GTPase, C3 exoenzyme, and by a Rho kinase inhibitor, Y27632. We previously showed that a small GTPase, RhoA, plays an important role in the peritoneal dissemination of ovarian carcinoma cells both *in vivo* and *in vitro*.[9] These findings suggest that the S100A4-RhoA signal is essential in the invasion of ovarian carcinoma cells, although its signal effect is not yet clearly understood. As Rho GTPase is known to be involved in cell motility, an association between S100A4 and cell motility is reasonable.[35] Noviskaya *et al.* reported that S100A4 stimulation was involved in the activation of both phospholipase C and protein kinase C.[16] A possible relationship between S100A4, matrix metalloproteinases, and invasive capacity has also been reported.[36,37] Extracellular function of S100A4 might also include angiogenesis.[17,38] Thus, further research is needed to clarify the intercellular and extracellular mechanisms of S100A4 involvement in the progression of ovarian carcinomas.

doi: 10.1111/j.1349-7006.2006.00295.x

In summary, the cytoplasmic and nuclear expression of S100A4 is stronger in ovarian carcinomas than in benign or borderline tumors, and nuclear expression of S100A4 could be an indicator for poor prognosis in ovarian carcinoma patients. In addition, ovarian carcinoma cells express S100A4 at the mRNA and protein levels and secrete S100A4, which might in turn work for its own upregulation as well as its nuclear translocation, along with an enhancement of invasiveness *in vitro*. Thus, S100A4 might be an important autocrine/paracrine factor involved in the aggressive characteristics of ovarian carcinoma cells, and could be a molecular target in the treatment of ovarian carcinoma. Development of a novel therapy targeted to the S100A4-RhoA pathway is needed to improve the survival of ovarian carcinoma patients.

Acknowledgments

This work was supported in part by Grants-in-Aid for Scientific Research from the Ministry of Education, Science and Culture (No. 15390502, No. 16790947), Japan.

References

1 Murdoch WJ. Ovarian surface epithelium, ovulation and carcinogenesis. *Biol Rev Camb Philos Soc* 1996; **71**: 529–43.
2 Mandai M, Konishi I, Komatsu T *et al.* Mutation of the *nm23* gene, loss of heterozygosity at the *nm23* locus and K-ras mutation in ovarian carcinoma: correlation with tumour progression and *nm23* gene expression. *Br J Cancer* 1995; **72**: 691–5.
3 Imai T, Horiuchi A, Wang C *et al.* Hypoxia attenuates the expression of E-cadherin via up-regulation of SNAIL in ovarian carcinoma cells. *Am J Pathol* 2003; **163**: 1437–47.
4 Bernstein LR, Liotta LA. Molecular mediators of interactions with extracellular matrix components in metastasis and angiogenesis. *Curr Opin Oncol* 1994; **6**: 106–13.
5 Schmalfeldt B, Prechtel D, Harting K *et al.* Increased expression of matrix metalloproteinases (MMP)-2, MMP-9, and the urokinase-type plasminogen activator is associated with progression from benign to advanced ovarian cancer. *Clin Cancer Res* 2001; **7**: 2396–404.
6 Baserga R. Oncogenes and the strategy of growth factors. *Cell* 1994; **79**: 927–30.
7 Yamamoto S, Konishi I, Mandai M *et al.* Expression of vascular endothelial growth factor (VEGF) in epithelial ovarian neoplasms: correlation with clinicopathology and patient survival, and analysis of serum VEGF levels. *Br J Cancer* 1997; **76**: 1221–7.
8 Horiuchi A, Imai T, Shimizu M *et al.* Hypoxia-induced changes in the expression of VEGF, HIF-1 alpha and cell cycle-related molecules in ovarian cancer cells. *Anticancer Res* 2002; **22**: 2697–702.
9 Horiuchi A, Imai T, Wang C *et al.* Up-regulation of small GTPases, RhoA and RhoC, is associated with tumor progression in ovarian carcinoma. *Laboratory Invest* 2003; **83**: 861–70.
10 Donato R. S100: a multigenic family of calcium-modulated proteins of the EF-hand type with intracellular and extracellular functional roles. *Int J Biochem Cell Biol* 2001; **33**: 637–68.
11 Selinfreund RH, Barger SW, Welsh MJ, Van Eldik LJ. Antisense inhibition of glial S100 beta production results in alterations in cell morphology, cytoskeletal organization, and cell proliferation. *J Cell Biol* 1990; **111**: 2021–8.
12 Davies BR, Davies MP, Gibbs FE, Barraclough R, Rudland PS. Induction of the metastatic phenotype by transfection of a benign rat mammary epithelial cell line with the gene for p9Ka, a rat calcium-binding protein, but not with the oncogene EJ-ras-1. *Oncogene* 1993; **8**: 999–1008.
13 Davies MP, Rudland PS, Robertson L, Parry EW, Jolicoeur P, Barraclough R. Expression of the calcium-binding protein S100A4 (p9Ka) in MMTV-neu transgenic mice induces metastasis of mammary tumors. *Oncogene* 1996; **13**: 1631–7.
14 Parker C, Whittaker PA, Usmani BA, Lakshmi MS, Sherbet GV. Induction of 18A2/mts1 gene expression and its effects on metastasis and cell cycle control. *DNA Cell Biol* 1994; **13**: 1021–8.
15 Ilg EC, Schafer BW, Heizmann CW. Expression pattern of S100 calcium-binding proteins in human tumors. *Int J Cancer* 1996; **68**: 325–2.
16 Novitskaya V, Grigorian M, Kriajevska M *et al.* Oligomeric forms of the metastasis-related Mts1 (S100A4): protein stimulate neuronal differentiation in cultures of rat hippocampal neurons. *J Biol Chem* 2000; **275**: 41278–86.
17 Semov A, Moreno MJ, Onichtchenko A *et al.* Metastasis-associated protein S100A4 induces angiogenesis through interaction with annexin II and accelerated plasmin formation. *J Biol Chem* 2005; **280**: 20833–41.
18 Mueller A, Bachi T, Hochli M, Schafer BW, Heizmann CW. Subcellular distribution of S100 proteins in tumor cells and their relocation in response to calcium activation. *Histochem Cell Biol* 1999; **111**: 453–9.
19 Silverberg SG. Histopathologic grading of ovarian carcinoma: a review and proposal. *Int J Gynecol Pathol* 2000; **19**: 7–15.
20 Scully RE, Young RH, Clement PB. Surface epithelial-stromal tumors and serous tumors. In: Rosai J, Sobin LH, eds. *Atlas of Tumor Pathology. Tumors of the Ovary, Maldeveloped Gonads, Fallopian Tube, and Broad Ligament.* Third series, Fascicle 23. Washington DC: Armed Forces Institute of Pathology, 1998.
21 Davies BR, O'Donnell M, Durkan GC *et al.* Expression of S100A4 protein is associated with metastasis and reduced survival in human bladder cancer. *J Pathol* 2002; **196**: 292–9.
22 Pedersen KB, Nesland JM, Fodstad O, Maelandsmo GM. Expression of S100A4, E-cadherin, alpha- and beta-catenin in breast cancer biopsies. *Br J Cancer* 2002; **87**: 1281–6.
23 Tsuruo T, Hamilton TC, Louie KG, Behrens BC, Young RC, Ozols RF. Collateral susceptibility of adriamycin-, melphalan- and cisplatin-resistant human ovarian tumor cells to bleomycin. *Jpn J Cancer Res* 1986; **77**: 941–5.
24 Chomczynski P, Sacchi N. Single-step method of RNA isolation by acid guanidinium thiocyanate-phenol-chloroform extraction. *Anal Biochem* 1987; **162**: 156–9.
25 Albini A, Iwamoto Y, Kleinman HK *et al.* A rapid *in vitro* assay for quantitating the invasive potential of tumor cells. *Cancer Res* 1987; **47**: 3239–45.
26 Ito T, Williams JD, Fraser D, Phillips AO. Hyaluronan attenuates transforming growth factor-beta1-mediated signaling in renal proximal tubular epithelial cells. *Am J Pathol* 2004; **164**: 1979–88.
27 Bjornland K, Winberg JO, Odegaard OT *et al.* S100A4 involvement in metastasis: deregulation of matrix metalloproteinases and tissue inhibitors of matrix metalloproteinases in osteosarcoma cells transfected with an anti-S100A4 ribozyme. *Cancer Res* 1999; **59**: 4702–8.
28 Sato N, Fukushima N, Maitra A *et al.* Gene expression profiling identifies genes associated with invasive intraductal papillary mucinous neoplasms of the pancreas. *Am J Pathol* 2004; **164**: 903–14.
29 Rudland PS, Platt-Higgins A, Renshaw C *et al.* Prognostic significance of the metastasis-inducing protein S100A4 (p9Ka) in human breast cancer. *Cancer Res* 2000; **60**: 1595–603.
30 Hsieh HL, Schafer BW, Weigle B, Heizmann CW. S100 protein translocation in response to extracellular S100 is mediated by receptor for advanced glycation endproducts in human endothelial cells. *Biochem Biophys Res Commun* 2004; **316**: 949–59.
31 Sakaguchi M, Miyazaki M, Inoue Y *et al.* Relationship between contact inhibition and intranuclear S100C of normal human fibroblasts. *J Cell Biol* 2000; **149**: 1193–206.
32 Davey GE, Murmann P, Heizmann CW. Intracellular Ca^{2+} and Zn^{2+} levels regulate the alternative cell density-dependent secretion of S100B in human glioblastoma cells. *Biol Chem* 2001; **276**: 30819–26.
33 Flatmark K, Pedersen KB, Nesland JM *et al.* Nuclear localization of the metastasis-related protein S100A4 correlates with tumour stage in colorectal cancer. *J Pathol* 2003; **200**: 589–95.
34 Mandinova A, Atar D, Schafer BW, Spiess M, Aebi U, Heizmann CW. Distinct subcellular localization of calcium binding S100 proteins in human smooth muscle cells and their relocation in response to rises in intracellular calcium. *J Cell Sci* 1998; **111**: 2043–54.
35 Jenkinson SR, Barraclough R, West CR, Rudland PS. S100A4 regulates cell motility and invasion in an *in vitro* model for breast cancer metastasis. *Br J Cancer* 2004; **90**: 253–62.
36 Schmidt-Hansen B, Ornas D, Grigorian M *et al.* Extracellular S100A4 (mts1) stimulates invasive growth of mouse endothelial cells and modulates MMP-13 matrix metalloproteinase activity. *Oncogene* 2004; **23**: 5487–95.
37 Mathisen B, Lindstad RI, Hansen J *et al.* S100A4 regulates membrane induced activation of matrix metalloproteinase-2 in osteosarcoma cells. *Clin Exp Metastasis* 2003; **20**: 701–11.
38 Ambartsumian N, Klingelhofer J, Grigorian M *et al.* The metastasis-associated Mts1 (S100A4): protein could act as an angiogenic factor. *Oncogene* 2001; **20**: 4685–95.

Adenovirus-Mediated *Calponin h1* Gene Therapy Directed against Peritoneal Dissemination of Ovarian Cancer: Bifunctional Therapeutic Effects on Peritoneal Cell Layer and Cancer Cells

Tomonori Ogura,[1] Hiroaki Kobayashi,[1] Yousuke Ueoka,[1] Kaoru Okugawa,[1] Kiyoko Kato,[2] Toshio Hirakawa,[1] Shigenari Hashimoto,[3,4] Shun'ichiro Taniguchi,[4] Norio Wake,[1] and Hitoo Nakano[1]

Abstract **Purpose:** Calponin h1 (CNh1), one of the family of actin-binding proteins, stabilizes the filaments of actin and modulates various cellular biological phenotypes. Recent studies revealed the close correlation between the invasive tumor spread and the reduced expression of CNh1 and α-smooth muscle actin in the surrounding stromal cells. The purpose of this study is to evaluate the efficacy of i.p. *CNh1* gene therapy against peritoneal dissemination of ovarian cancer.

Experimental Design: We used an adenoviral vector to induce the *CNh1* gene into peritoneal cells and ovarian cancer cells as a means of enhancing or inducing the expression of α-smooth muscle actin as well as CNh1. The efficacy of gene transfer was examined by *in vitro* cell culture and *in vivo* animal experiments.

Results: The formation of longer and thicker actin fibers was observed in each transfected cell line, and the localization of these fibers coincided with that of externally transducted *CNh1*. With respect to changes in cell behavior, the *CNh1*-transfected peritoneal cells acquired an ability to resist ovarian cancer-induced shrinkage in cell shape; thus, cancer cell invasion through the monolayer of peritoneal cells was inhibited. In addition, *CNh1*-transfected ovarian cancer cells showed suppressed anchorage-independent growth and invasiveness, the latter of which accompanied impaired cell motility. The concomitant *CNh1* transfection into both peritoneal cells and ovarian cancer cells produced an additive inhibitory effect with respect to cancer cell invasion through the peritoneal cell monolayer. By *in vivo* experiments designed to treat nude mice that had been i.p. inoculated with ovarian cancer cells, we found that the i.p. injected *CNh1* adenovirus successfully blocked cancer-induced morphologic changes in peritoneal cell surface and significantly prolonged the survival time of tumor-bearing mice. Moreover, *CNh1* adenovirus could successfully enhance the therapeutic effect of an anticancer drug without increase in side effects.

Conclusions: Thus, *CNh1* gene therapy against peritoneal dissemination of ovarian cancer is bifunctionally effective (i.e., through inhibitory effects on the infected peritoneal cell layers that suppress cancer invasion and through direct antitumor effects against invasion and growth properties of cancer cells).

Authors' Affiliations: [1]Department of Gynecology and Obstetrics, Graduate School of Medical Sciences, and [2]Department of Molecular Genetics, Division of Molecular and Cell Therapeutics, Medical Institute of Bioregulation, Kyushu University, Fukuoka, Japan; [3]Division of Otorhinolaryngology, Shinshu University School of Medicine, Matsumoto, Japan; and [4]Department of Molecular Oncology, Institute on Aging and Adaptation, Shinshu University Graduate School of Medicine, Matsumoto, Japan

Received 3/20/06; revised 6/8/06; accepted 6/15/06.

Grant support: Ministry of Education, Culture, Sports, Science, and Technology, Japan scientific research grants 14570117, 15390509, 16659100, 1690960, and 17591747.

The costs of publication of this article were defrayed in part by the payment of page charges. This article must therefore be hereby marked *advertisement* in accordance with 18 U.S.C. Section 1734 solely to indicate this fact.

Note: T. Ogura and H. Kobayashi contributed equally to this work.

Requests for reprints: Hiroaki Kobayashi, Department of Gynecology and Obstetrics, Graduate School of Medical Sciences, Kyushu University, Maidashi 3-1-1, Higashi-ku, Fukuoka 812-8582, Japan. Phone: 81-92-642-5395; Fax: 81-92-642-5414; E-mail: koba@med.kyushu-u.ac.jp.

doi:10.1158/1078-0432.CCR-06-0674

Peritoneal dissemination is a main obstacle to improve the prognosis of ovarian cancer patients. The process to establish peritoneal implants is as follows: cancer cells are released from the primary ovarian tumor site into the abdominal cavity, attach to and invade through the peritoneal mesothelial layer, and proliferate as "implanted" tumors. For these processes, dynamic cytoskeletal remodeling is essential not only for the tumor cells but also for the peritoneal cells. A recent study analyzing several adenocarcinomas of various organs has shown that nine genes in metastatic sites were universally down-regulated compared with their primary tumor counterparts (1). Surprisingly, four of these nine genes are associated with the actin cytoskeleton [i.e., α-actin, myosin light and heavy chain kinases, and calponin h1 (CNh1)]. As such, this seems to be a reflection of the importance of actin cytoskeletal disorganization in the metastatic process.

CNh1 is a 34-kDa actin-binding protein that was originally isolated from chicken gizzard (2). CNh1 is mainly expressed in

smooth muscle cells in contrast to other two isoforms of calponin h2 and acidic calponin, which are mainly expressed in nonmuscle cells and the brain, respectively (3–5). CNh1 has an ability to (*a*) bind to the thin filament of actin, tropomyosin, and calmodulin (2, 6, 7); (*b*) inhibit the actin-activated myosin Mg-ATPase (8); (*c*) inhibit Ca^{2+}-dependent mobility of actin on immobilized myosin (9); and (*d*) induce conformational changes in actin filament (F-actin; ref. 10). Therefore, CNh1 is thought to play an essential role in organizing stable actin stress fibers. We have confirmed previously that (*a*) the expression of α-smooth muscle actin (α-SMA) decreased in blood vessels located at the proximity of ovarian cancer nests (11) and in fibroblasts and peritoneal mesothelia cultured in the presence of ovarian cancer cell–derived factors[5] and (*b*) the decrease in CNh1 and α-SMA expression was seemingly attributed to the secreted factors, including platelet-derived growth factor derived from cancer cells (12, 13). *CNh1* knockout mice showed the enhanced peritoneal dissemination and lung metastasis by malignant melanoma cells through their highly fragile peritoneum and vascular wall in contrast to the wild-type mice. However, *CNh1* gene transfection into the peritoneal cells of knockout mice could successfully inhibit cancer cell invasion into peritoneal cell layer (14, 15). The efficacy of *CNh1* transfection into cancer cells themselves was also reported by our colleagues; both cell growth and tumorigenicity were significantly inhibited in *CNh1*-transfected leiomyosarcoma cells (16) and fibrosarcoma cells (17).

Based on these observations, we hypothesized that CNh1 has bifunctional effects (i.e., an enhancement of peritoneal defense ability on the one hand and a direct inhibitory effect against for ovarian cancer cells on the other). The purpose of this study was to examine the effects of *CNh1* gene transduction into both cancer cells and peritoneal cells with respect to inhibiting peritoneal dissemination of ovarian cancers.

Materials and Methods

Cell lines and animals. Four i.p. transplantable (SHIN-3, MCAS/as, OVAS-21/om, and SKOV3i.p.1) and a poorly transplantable (SKOV3) human ovarian cancer cell lines were used in this study. SHIN-3, a serous adenocarcinoma cell line, was purchased from Scienstaff Co. Ltd. (Nara, Japan). MCAS/as and OVAS-21/om were established from ascites and omentum of nude mice i.p. inoculated by their parental cell lines of MCAS (mucinous adenocarcinoma) and OVAS-21 (clear cell adenocarcinoma), respectively. Both cell lines were generous gifts from Drs. S. Minami and Y. Yoshikawa (Department of Obstetrics and Gynecology, University of Tsukuba, Japan) and M. Noguchi (Department of Molecular Pathology, University of Tsukuba). SKOV3i.p.1, provided by Dr. I.J. Fidler (Department of Cancer Biology, M.D. Anderson Cancer Center, Houston, TX), was established as an i.p. transplantable subline from a parental adenocarcinoma cell line of SKOV3 (18). A Chinese hamster peritoneal cell line, CCL14, was purchased from American Type Culture Collection (Manassas, VA). FK is a primary culture of human peritoneal cells, which were obtained from the surgical specimen of omentum under the patient's consent in Department of Obstetrics and Gynecology, Kyushu University Hospital. Each cell line was cultured in RPMI 1640 (Invitrogen, Carlsbad, CA) supplemented with 10% fetal bovine serum, 100 μg/mL streptomycin, 100 units/mL penicillin G, and 2.5 μg/mL amphotericin B at 37°C in 5% CO_2 in air.

Female athymic BALB/c *nu/nu* mice between 6 and 8 weeks old (Charles River Japan, Atsugi, Japan) were used for *in vivo* experiments. The mice were maintained in a laminar-flow cabinet under specific pathogen-free conditions while receiving standard feed and water *ad libitum*. Our experiments were reviewed by the Committee of Ethics in Animal Experiments in the Graduate School of Medical Sciences, Kyushu University, and the Law (no. 105) and the Notification (no. 6) of the Government.

Construction of recombinant adenovirus and adenoviral gene transfection into cultured cells. Recombinant adenovirus was inserted with the *CNh1*-green fluorescent protein (GFP) fusion gene (AdCNh1) or with the *GFP* gene only (AdGFP, control vector) as described previously (15). Briefly, *CNh1-GFP* fusion gene was produced by inserting human *CNh1* gene into pEGFP-C2 (Clontech, Palo Alto, CA), and then subcloned under the transcriptional control of CAG promoter/enhancer in cosmid vector pAxCAwt (adenovirus expression kit, TaKaRa, Japan; Fig. 1). The recombinant was continued in 293 cells by four times infection and high titer virus was obtained. Adenoviral infection into the cells was carried out by incubating subconfluent cells with adenoviral vectors (2×10^7 plaque-forming units/15-mm dish) for 2 hours in RPMI 1640 at 37°C. Cells were then washed twice with PBS and the medium was changed into RPMI 1640 containing 10% fetal bovine serum. After 24 hours of incubation, cells were used for immunofluorescent cell staining and colony-forming assay. For Western blot analysis, *in vitro* invasion assay, and cell motility assay, cells were used after 4 days of additional incubation.

Plasmid gene transfection into cultured cells. A human *CNh1* cDNA was subcloned into a pCMV-neo-Bam vector as described previously (17). Either *CNh1* cDNA construct or control vector (20 μg) was transfected into SKOV3 cell line by Lipofectin method. Transfected cells were maintained at 37°C in a complete RPMI 1640. After 14 days, the G418-resistant clones were harvested and established.

Western blot analysis. Subconfluently growing cells were lysed in a lysis buffer [50 mmol/L Tris-HCl (pH 8.0), 0.25 mol/L NaCl, 0.5% NP40, 1 mmol/L phenylmethylsulfonyl fluoride, 10 μg/mL aprotinin, 1 μg/mL leupeptin]. After centrifugation at 13,000 × *g* for 10 minutes to remove debris, equal protein amount of cell lysates was separated on

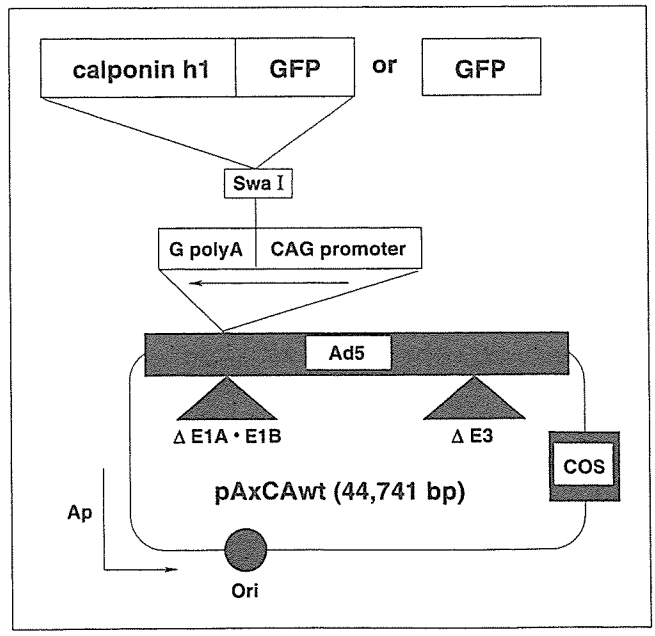

Fig. 1. Construction of *CNh1-GFP* recombinant adenovirus vector (AdCNh1) and its control *GFP* vector (AdGFP).

[5] Unpublished observations.

SDS-PAGE and transferred onto nitrocellulose membranes. The membranes were blocked in TBS [10 mmol/L Tris-HCl (pH 7.4), 150 mmol/L NaCl, 0.05% Tween 20] containing 5% nonfat dry milk for 1 hour at room temperature and washed in TBS-Tween 20 for 5 minutes. The blots were incubated with anti-human CNh1 monoclonal antibody (Sigma, St. Louis, MO), anti-human α-SMA monoclonal antibody (Progen, Queensland, Australia), anti-β-actin monoclonal antibody (Sigma), antibody (Santa Cruz Biotechnology, Inc., CA) for 2 hours at room temperature. After washing, the blots were reacted with their respective secondary antibodies (Amersham, Piscataway, NJ) and analyzed with enhanced chemiluminescence system (Amersham). All primary antibodies are informed to detect CNh1 protein stably even in murine tissues.

Immunofluorescent cell staining for F-actin. Cells were washed with PBS and fixed in 3.7% formaldehyde solution in PBS for 10 minutes at room temperature. After permeabilization with 1% Triton X-100, the rhodamine-phalloidin (Molecular Probes, OR) diluted with 0.1% bovine serum albumin in PBS was added and incubated at room temperature for 20 minutes. F-actin and GFP were observed with confocal laser scanning microscope using specific filters for rhodamine and FITC, respectively.

Soft-agar colony-forming assay. After 24 hours of infection with AdCNh1 or AdGFP, 10^4 cells were seeded into the complete medium, including 0.3% agar, and placed over a hardened 0.5% agar base layer in 60-mm dishes. Visible colonies were counted in triplicate after 14 days of incubation to evaluate the anchorage-independent cell growth.

Tumorigenicity in nude mice. Single-cell suspension containing 10^7 SKOV3 cells with or without plasmid transfection was i.m. injected into the thigh of nude mice. The mice were observed weekly, and tumor growth was evaluated by measuring the thickness of the inoculated thigh.

Cell motility assay. Cell motility was determined using Transwell chambers inserted with 8-μm pore size membrane (Costar, Corning, NY) according to the method described previously (19). Each lower compartment of Transwell chambers was filled with a conditioned medium as a source of chemoattractant, which was a supernatant of confluently cultured NIH3T3 cells in DMEM supplemented with 10% fetal bovine serum for 24 hours. Single-cell suspension containing 5×10^4 cells infected by AdCNh1 or AdGFP in 100 μL RPMI 1640 with 0.1% bovine serum albumin was placed in its upper compartment. The cells were incubated for 12 hours at 37°C, fixed with methanol, and stained with H&E. Cells on the upper surface of the filter were removed with a cotton swab, and cells that migrated to the lower surface were counted by six fields of a light microscope at ×200 magnification.

In vitro *invasion assay.* *In vitro* invasion assay was done using Transwell chambers with 8-μm pore membrane coated with 20 μg Matrigel (Becton Dickinson Collaborative Research, Bedford, MA) as described previously (20). Conditioned medium prepared by NIH3T3 cells was placed in the lower compartment. Single-cell suspension containing 10^5 cells in 100 μL RPMI 1640 containing 10% fetal bovine serum was placed in the upper compartment and incubated for 24 hours. The subsequent procedures were the same as those of the cell motility assay.

Assay for invasion through the peritoneal cell monolayer. Single-cell suspensions containing 10^6 cancer cells infected with AdCNh1 or AdGFP were plated on the monolayer of CCL14 peritoneal cells infected with AdCNh1 or AdGFP, and cultured for additional 24 hours. The number of colonies derived from a penetrated cancer cell was counted by six fields of a phase-contrast microscope at ×400 magnification.

Therapeutic experiments against i.p. inoculated ovarian cancer cells. One day after the inoculation of 10^6 cells of OVAS-21/om, the i.p. injection of AdCNh1 or AdGFP (2×10^8 plaque-forming units/2 mL) was started and repeated by every 3 days until 19 days after the inoculation. In some groups, 100 mg/kg paclitaxel was given once i.p. at 3 days after inoculation. Survival and body weight of each mouse were monitored until 5 months after the inoculation, and an autopsy was done. Paclitaxel (Taxol) was kindly provided by Bristol-Myers Squibb (Tokyo, Japan).

Scanning electron microscope. Peritoneum was resected from abdominal walls of mice at 7 days after the i.p. inoculation of SKOV3i.p.1 cancer cells followed by the adenoviral injection. Peritoneal tissues were fixed in 1% glutaraldehyde for 12 hours followed by 1-hour fixation in 1% osmium tetroxide. After dehydration in ethanol, the specimens were rinsed in isoamyl acetate and dried by a critical point drying method. The dried specimens were mounted on copper plates and coated with osmium in an osmium plasma coater (Nippon Laser and Electronics Lab, Japan). The specimens were examined with a JSM-6000F scanning electron microscope (Jeol, Pleasonton, CA) at 1.5 kV.

Statistical analysis. Mann-Whitney *U* test was used to assess the statistical significance of differences in soft-agar colony-forming assay, cell motility assay, *in vitro* invasion assay, and assay for cell invasion through the peritoneal cell layer. *In vivo* tumor growth assay was assessed using Fisher's exact test. Survival curves were analyzed with Kaplan-Meier method and the difference between curves was assessed according to the log-rank test. All *P*s are two-sided and considered statistically significant at <0.05.

Results

Efficacy of *CNh1* gene transfection into the peritoneal cells

Expression of CNh1 and three kinds of actin proteins in the transfected peritoneal cells. Although endogenous expression of 34-kDa CNh1 protein was found in CCL14 cells infected with AdGFP or AdCNh1 (Fig. 2A) as well as noninfected CCL14 cells, exogenous CNh1 protein fused with GFP appeared additionally as a 61-kDa band in AdCNh1-infected cells (Fig. 2A). Because CNh1 is known to stabilize α-SMA, the expressions of α, β, and γ actin proteins were analyzed after *CNh1* adenoviral infection. No change of expression of any actin was observed between AdGFP-infected cells and their parental noninfected cells. Although expression of β and γ actins were not changed even by AdCNh1 infection, α-SMA expression was clearly enhanced by *CNh1* transfection (Fig. 2A and B).

Effects of CNh1 *gene transfection into the peritoneal cells against the destabilization of their actin filaments in the presence of conditioned medium of ovarian cancer cells.* Original peritoneal cells show well-developed actin stress fibers within their cytoplasm and well-stretched cell shape in normal culture medium. In the presence of ovarian cancer conditioned medium, we observed decreased actin stress fibers resulting in shrunken cell shape, intercellular dissociation, and cell detachment from culture plate, and this phenomenon was specifically accompanied by decreasing expressions of both CNh1 and α-SMA.[5] Therefore, we examined whether *CNh1* transfection into the peritoneal cells could stabilize actin filaments against the ovarian cancer-derived factors. As shown in Fig. 3A, AdGFP-infected cells in the presence of ovarian cancer conditioned medium showed smaller and shrunken cell shape with thin and short actin filaments at the cytosol and small spike-like filaments observed at the cellular margins, which is similar in appearance to the noninfected FK cells in the presence of ovarian cancer conditioned medium. Therefore, AdGFP infection could not recover the FK cells from ovarian cancer-derived morphologic changes. On the other hand, AdCNh1-infected cells maintained large and extended cell shape with thick and long filaments traversing a cell, just like untreated parental peritoneal cells, even in the presence of ovarian cancer conditioned medium (Fig. 3B). Localization of actin stress fiber (Fig. 3B) was identical with the expression site of *CNh1-GFP* gene products (Fig. 3C), which was